Letters to the Editor

Elevation of B cell-activating factor belonging to the tumour necrosis factor family (BAFF) in haemophilia A patients with inhibitor

Tomohiro Takeda[1,2]; Yoshihiko Sakurai[1]; Kohei Tatsumi[1]; Junko Kato[1]; Shogo Kasuda[1]; Akira Yoshioka[1]; Midori Shima[1]

[1]Department of Pediatrics, Nara Medical University School of Medicine, Kashihara, Japan;
[2]Clinical Laboratory, Uda General Hospital, Uda, Japan

Dear Sir,

The development of factor VIII (FVIII) neutralizing antibodies (inhibitors) is one of the serious complications in the clinical management of haemophilia A. As replacement therapy with FVIII concentrates is ineffective or markedly impaired in this setting, the management of inhibitor patients is full of difficulty. Although FVIII inhibitor will develop by both B cell- and T cell-dependent immune system (1, 2), the precise immune regulatory mechanism of inhibitors has not been fully addressed.

Recently, new ligands, BAFF (B cell-activating factor belonging to the tumour necrosis factor [TNF] family, also known as BlyS) and APRIL (a proliferation inducing ligand), have been found to regulate immune system. BAFF is a member of the TNF superfamily of ligands and is involved in the survival and maturation of B cells (3). Another member of the superfamily, APRIL, also stimulates B- and T-cell proliferation and triggers humoral immune responses (4). BAFF binds to the TNF-related receptors such as B-cell maturation antigen (BCMA), transmembrane activator and calcium modulator and cyclophilin ligand interactor (TACI) and BAFF receptor (BAFFR), whereas APRIL binds to TACI and BCMA and to heparan-sulfate proteoglycans (5). Such BAFF/APRIL ligand-TNF related receptor interaction comprises a complex network that is critically involved in the induction and regulation of humoral immunity. We hypothesized that BAFF and/or APRIL would participate in the development and preservation of inhibitors. To test the hypothesis, we measured BAFF and APRIL levels in haemophilia A patients with and without inhibitors.

Citrated plasma samples were obtained from 25 healthy individuals and 21 haemophilia A patients without inhibitors. Sixteen samples were from eight haemophilia A patients with inhibitors at different times. Mean (± standard deviation [SD]) historical peak inhibitor titers were 420.2 ± 877.8 BU/ml (range 8.2–2586). Inhibitors had been present at least for nine months when sample plasma was taken. All haemophilia A patients with and without inhibitors were diagnosed in our laboratory as severe or moderate type haemophilia A. Since BAFF level is significantly increased in patients with chronic hepatitis C virus (HCV) (6), haemophilia A patients with HCV infection were not enrolled in this study.

Plasma BAFF and APRIL levels were measured using specific ELISA kits (R&D Systems, Minneapolis, MN, USA and Bender MedSystems, Burlingame, CA, USA, respectively). Each sample was tested in duplicate. Total plasma IgG was also measured with a standard immunoturbidimetric test. Statistical analysis was performed using unpaired t-tests between groups.

Mean (± SD) inhibitor titer in haemophilia A patients with inhibitors was 104.0 ± 191.9 BU/ml (range 1.2–742). Mean (± SD) age of healthy individuals was 16.7 ± 14.0 years (range 1–42), that of haemophilia A patients without inhibitors was 15.0 ± 6.1 years (range 4–26), and that of haemophilia A patients with inhibitors was 9.4 ± 10.6 years (range 3–44). There was no significant difference in age among these groups.

In non-haemophiliac individuals (n=19), the plasma levels of BAFF and APRIL correlated well with those of serum ($p<0.001$, $R^2=0.92$; $p<0.001$, $R^2=0.94$, respectively), confirming the validation of these assays using citrated plasma samples.

Mean plasma BAFF levels (± SD) were significantly higher in haemophilia A patients with inhibitors (896 ± 191.4 pg/ml, range 594–1,399) than in healthy controls (746 ± 220 pg/ml, range 375–1,269) ($p<0.05$) and in haemophilia A without inhibitors (751 ± 236 pg/ml, range 352–1,056) ($p<0.05$) (Fig. 1, left). There was no significance between BAFF levels in healthy controls and in haemophilia A patients without inhibitors ($p=0.938$). In APRIL levels, no significance was observed between in healthy controls (10.0 ± 7.5 ng/ml, range 0.4–24.0) and in haemophilia A patients without inhibitors (8.2 ± 6.1 ng/ml, range 0.0–17.4) ($p=0.415$), between in healthy controls and in haemophilia A patients with inhibitors (15.1 ± 15.6 ng/ml, range 0.1–51.3) ($p=0.169$), and between in haemophilia A patients without inhibitors and those with inhibitors ($p=0.101$). These results suggest that BAFF is involved in the regulation of immunological response toward preservation of inhibitor. Meanwhile, significant differences of BAFF/APRIL levels were not observed between severe type and moderate type of haemophilia A (data not shown). No evident correlation between BAFF/APRIL

Correspondence to:
Yoshihiko Sakurai, MD, PhD
Department of Pediatrics, Nara Medical University
840 Shijo-cho, Kashihara, Nara 634–8522, Japan
Tel.: +81 744 29 8881, Fax: +81 744 24 9222
E-mail: ysakurai@naramed-u.ac.jp

Financial support:
This work was partially supported by grants from the Kurozumi Medical Foundation and Mitsubishi Pharma Research Foundation to YS, and by Health and Labor Sciences Research Grants (Research on Regulatory Science of Pharmaceuticals and Medical Devices, and Research on HIV/AIDS) from Ministry of Health, Labor, and Welfare, Japan to AY.

Received: August 23, 2008
Accepted after minor revision: November 12, 2008

Prepublished online: January 15, 2009
doi:10.1160/TH08-08-0543

Thromb Haemost 2009; 101: 408–410

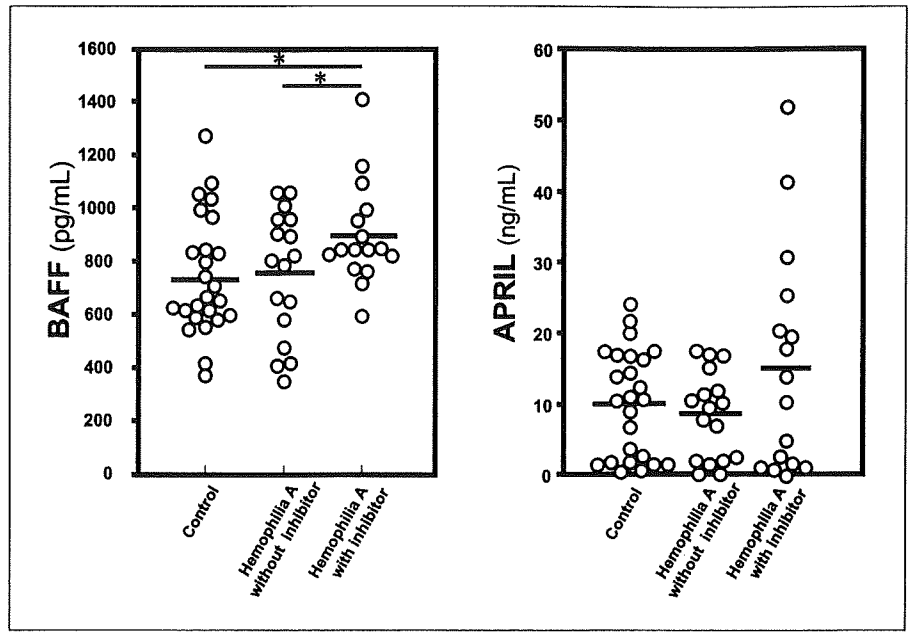

Figure 1: Plasma BAFF and APRIL levels in healthy controls, haemophilia A patients without inhibitors, and haemophilia A patients with inhibitors. Bars represent mean. Left: Plasma BAFF levels. Right: Plasma APRIL levels. *: $p<0.05$.

level and inhibitor titer, historical peak, and duration of inhibitor was confirmed (data not shown). Total IgG levels were within normal range consistent with age in all haemophilia A patients (data not shown). No correlation was observed between BAFF and IgG levels in haemophilia A patients with and without inhibitors (data not shown), suggesting that elevated BAFF levels in haemophilia A patients with inhibitors were insufficient for aberrant elevation of total IgG. Further IgG subclass analysis will be helpful to investigate the role of BAFF in inhibitor preservation as BAFF might induce IgG subclass switch.

Previous mouse studies demonstrated that constitutive BAFF overexpression results in the survival of autoreactive B cells (3, 7, 8), leading to a breakdown of peripheral tolerance. In this setting, autoimmune disorders develop in mice through aberrant activation of B cells, spontaneous production of multiple autoantibodies and polyclonal hypergammaglobulinaemia. In humans, elevated BAFF levels are correlated with hypergammaglobulinaemia and several B cell-mediated autoimmune diseases (9–11). Previous studies showed that anti-FVIII antibodies in the circulation and anti-FVIII antibody-secreting cells in the spleen and bone marrow persist for a long time even after termination of FVIII treatment (12). In haemophilia A patients with inhibitors, elevated BAFF levels would allow anti-FVIII antibody-secreting plasma cells to survive and produce inhibitors.

On the other hand, APRIL levels showed little difference among healthy controls, haemophilia A patients without inhibitors, and those with inhibitors. Although APRIL promotes IgA and IgG1 class switching in mouse IgM^+IgD^+ B cells (13), elevated APRIL levels in some haemophilia A patients with inhibitors remains of unknown significance. Further investigations will be required to address the role of APRIL in the haemophilia A patients with inhibitors.

Hitherto, congenital haemophilia A patients with inhibitors have received fewer B cell-targeted therapies such as rituximab therapy (14, 15) than acquired haemophilia (16). Treatment with a BAFF antagonist such as belimumab, a fully human monoclonal antibody that specifically binds to and neutralizes BAFF, was started in rheumatoid arthritis patients and demonstrated safety and efficacy (17). Targeting BAFF may represent a new therapeutic strategy in a subset of haemophilia A patients with refractory inhibitors presenting elevated BAFF levels.

References

1. Qian J, Borovok M, Bi L, et al. Inhibitor antibody development and T cell response to human factor VIII in murine haemophilia A. Thromb Haemost 1999; 81: 240–244.
2. Lavigne-Lissalde G, Schved JF, Granier C, et al. Anti-factor VIII antibodies: a 2005 update. Thromb Haemost 2005; 94: 760–769.
3. Mackay F, Browning JL. BAFF: a fundamental survival factor for B cells. Nat Rev Immunol 2002; 2: 465–475.
4. Dillon SR, Gross JA, Ansell SM, et al. An APRIL to remember: novel TNF ligands as therapeutic targets. Nat Rev Drug Discov 2006; 5: 235–246.
5. Bischof D, Elsawa SF, Mantchev G, et al. Selective activation of TACI by syndecan-2. Blood 2006; 107: 3235–3242.
6. Toubi E, Gordon S, Kessel A, et al. Elevated serum B-Lymphocyte activating factor (BAFF) in chronic hepatitis C virus infection: association with autoimmunity. J Autoimmun 2006; 27: 134–139.
7. Lesley R, Xu Y, Kalled SL, et al. Reduced competitiveness of autoantigen-engaged B cells due to increased dependence on BAFF. Immunity 2004; 20: 441–453.
8. Thien M, Phan TG, Gardam S, et al. Excess BAFF rescues self-reactive B cells from peripheral deletion and allows them to enter forbidden follicular and marginal zone niches. Immunity 2004; 20: 785–798.
9. Bosello S, Pers JO, Rochas C, et al. BAFF and rheumatic autoimmune disorders: implications for disease

management and therapy. Int J Immunopathol Pharmacol 2007; 20: 1–8.
10. Groom J, Kalled SL, Cutler AH, et al. Association of BAFF/BLyS overexpression and altered B cell differentiation with Sjogren's syndrome. J Clin Invest 2002; 109: 59–68.
11. Migita K, Abiru S, Maeda Y, et al. Elevated serum BAFF levels in patients with autoimmune hepatitis. Hum Immunol 2007; 68: 586–591.
12. Hausl C, Maier E, Schwarz HP, et al. Long-term persistence of anti-factor VIII antibody-secreting cells in haemophilic mice after treatment with human factor VIII. Thromb Haemost 2002; 87: 840–845.
13. Castigli E, Scott S, Dedeoglu F, et al. Impaired IgA class switching in APRIL-deficient mice. Proc Natl Acad Sci USA 2004; 101: 3903–3908.
14. Mathias M, Khair K, Hann I, et al. Rituximab in the treatment of alloimmune factor VIII and IX antibodies in two children with severe haemophilia. Br J Haematol 2004; 125: 366–368.
15. Carcao M, St Louis J, Poon MC, et al. Rituximab for congenital haemophiliacs with inhibitors: a Canadian experience. Haemophilia 2006; 12: 7–18.
16. Collins PW. Treatment of acquired haemophilia A. J Thromb Haemost 2007; 5: 893–900.
17. Cohen SB. Updates from B cell trials: efficacy. J Rheumatol (Suppl) 2006; 77: 12–17.

THE JOURNAL OF BIOLOGICAL CHEMISTRY VOL. 284, NO. 6, pp. 3379–3388, February 6, 2009

The Factor VIIIa C2 Domain (Residues 2228–2240) Interacts with the Factor IXa Gla Domain in the Factor Xase Complex*

Received for publication, June 30, 2008, and in revised form, October 30, 2008 Published, JBC Papers in Press, December 1, 2008, DOI 10.1074/jbc.M804955200

Tetsuhiro Soeda[‡], Keiji Nogami[‡], Katsumi Nishiya[‡], Masahiro Takeyama[‡], Kenichi Ogiwara[‡], Yoichi Sakata[§], Akira Yoshioka[‡], and Midori Shima[‡1]

From the [‡]Department of Pediatrics, Nara Medical University, Kashihara, Nara 634-8522, Japan and the [§]Division of Cell and Molecular Medicine, Center for Molecular Medicine, Jichi Medical University, Tochigi-ken 329-0498, Japan

Factor VIIIa functions as a cofactor for factor IXa in the phospholipid surface-dependent activation of factor X. Both the C2 domain of factor VIIIa and the Gla domain of factor IXa are involved in phospholipid binding and are required for the activation of factor X. In this study, we have examined the close relationship between these domains in the factor Xase complex. Enzyme-linked immunosorbent assay-based and surface plasmon resonance-based assays in the absence of phospholipid showed that Glu-Gly-Arg active site-modified factor IXa bound to immobilized recombinant C2 domain (rC2) dose-dependently (K_d = 108 nM). This binding ability was optimal under physiological conditions. A monoclonal antibody against the Gla domain of factor IXa inhibited binding by ~95%, and Gla domainless factor IXa failed to bind to rC2. The addition of monoclonal antibody or rC2 with factor VIIIa inhibited factor IXa-catalyzed factor X activation in the absence of phospholipid. Inhibition was not evident, however, in similar experiments in the absence of factor VIIIa, indicating that the C2 domain interacted with the Gla domain of factor IXa. A fragment designated C2-(2182–2259), derived from V8 protease-cleaved rC2, bound to Glu-Gly-Arg active site-modified factor IXa. Competitive assays, using overlapping synthetic peptides encompassing residues 2182–2259, demonstrated that peptide 2228–2240 significantly inhibited both this binding and factor Xa generation, independently of phospholipid. Our results indicated that residues 2228–2240 in the factor VIIIa C2 domain constitutes an interactive site for the Gla domain of factor IXa. The findings provide the first evidence for an essential role for this interaction in factor Xase assembly.

Factor VIII, a plasma protein that participates in the blood coagulation cascade, is deficient or defective in individuals with hemophilia A. Factor VIII circulates in plasma as a noncovalent complex with VWF,[2] which stabilizes the synthesis and activity of the cofactor. Mature factor VIII is synthesized as a single chain polypeptide of ~300 kDa consisting of 2,332 amino acid residues (1, 2). Based on internal homologies of the amino acid sequence, factor VIII has three types of domains arranged in the order of A1-A2-B-A3-C1-C2 (3). Factor VIII circulates in the plasma as a heterodimer of a heavy chain, consisting of the A1, A2, and heterogeneous fragments of partially proteolyzed B domains, together with a light chain consisting of the A3, C1, and C2 domains (1, 3).

The carboxyl-terminal 159 amino acids of factor VIII comprise the C2 domain, which is involved in binding to both VWF (4–6) and phospholipid membrane surfaces (6, 7). Binding in this domain appears to be competitive and mutually exclusive (4, 5, 8, 9). The C2 domain has also been shown to participate in binding to factor Xa and thrombin (10, 11). Additionally, a major epitope for allo- and autoantibodies and for monoclonal antibodies has been located within the C2 domain (4, 6, 12), indicating that this region could be an antigenic "hot spot." Consequently, important aspects of the expression and regulation of factor VIII appear to be governed by the structure and function of the C2 domain.

Factor VIIIa functions as a cofactor for factor IXa in the anionic, phospholipid surface-dependent conversion of factor X to Xa. In intrinsic factor Xase, factor VIIIa binds to factor IXa and increases the k_{cat} for factor Xa formation by several orders of magnitude compared with factor IXa alone (13). The A2 domain of factor VIIIa interacts with the catalytic domain of factor IXa, and the A3 domain interacts with the first epidermal growth factor domain (14). Although the affinity of isolated A2 for factor IXa is low (K_d ~ 300 nM), it amplifies the enzyme activity of factor IXa by modulating an active site in the catalytic domain, and this interaction defines the cofactor activity of factor VIIIa (15). Factor IXa-interactive sites in the A2 domain are located in at least three regions, within residues 484–509 (16), 558–565 (17), and 708–717 (18), respectively.

In contrast, the high affinity (K_d ~ 15 nM) of the isolated factor VIIIa light chain for factor IXa provides the majority of the binding energy for this interaction. To date, one region within the A3 domain, residues 1804–1818, has been identified

* This work was supported in part by MEXT KAKENHI Grant 19591264 and the Mitsubishi Pharma Research Foundation. A preliminary account of this work was presented at the 49th Annual Meeting of the American Society of Hematology, December 9, 2007, Atlanta, GA. The costs of publication of this article were defrayed in part by the payment of page charges. This article must therefore be hereby marked "*advertisement*" in accordance with 18 U.S.C. Section 1734 solely to indicate this fact.

[1] To whom correspondence should be addressed: Dept. of Pediatrics, Nara Medical University, 840 Shijo-cho, Kashihara, Nara 634-8522, Japan. Tel.: 81-744-29-8881; Fax: 81-744-24-9222; E-mail: roc-noga@naramed-u.ac.jp.

[2] The abbreviations used are: VWF, von Willebrand factor; Gla, γ-carboxyglutamic acid; rC2, recombinant C2 domain; HRP, horseradish peroxidase; GDless, Gla domainless; EGR-ck, Glu-Gly-Arg-chloromethylketone; HPLC, high performance liquid chromatography; LC/MS, liquid chromatography coupled to mass spectrometry; EGR-factor IXa, Glu-Gly-Arg active site-modified factor IXa; EGR-GDless factor IXa, Glu-Gly-Arg active site-modified Gla domainless factor IXa; BSA, bovine serum albumin; SPR, surface plasmon resonance; ELISA, enzyme-linked immunosorbent assay; mAb, monoclonal antibody.

as a factor IXa-interactive site (19, 20). Recently, Blostein *et al.* (21) demonstrated that the light chain of factor VIIIa interacts with the Gla domain of factor IXa, which contains 12 post-translationally modified glutamic acid residues (γ-carboxyglutamic acid) and functions in calcium-dependent phospholipid binding (22). However, the site in the light chain of factor VIIIa responsible for interaction with the Gla domain of factor IXa remains to be identified. The C2 domain of factor VIIIa and the Gla domain of factor IXa are involved in phospholipid binding, and both bound sequences could be aligned structurally close. We speculated, therefore, that the C2 domain of factor VIIIa might interact with the Gla domain of factor IXa in the factor Xase complex.

In the present study, we have examined the interaction between the C2 domain of factor VIIIa and the Gla domain of factor IXa in the factor Xase complex, using a combination of functional and binding assays employing recombinant C2 domain (rC2), V8 protease-digested C2 fragments, synthetic peptides, and monoclonal antibodies. Our results indicated that residues 2228–2240 in the C2 domain contain an interactive site for the Gla domain of factor IXa. The findings provide the first evidence for an essential role of this interaction in factor Xase assembly.

MATERIALS AND METHODS

Reagents—Purified recombinant factor VIII was a generous gift from Bayer Corp. (Osaka, Japan). Two monoclonal antibodies, mAb IXa-GD, against the Gla domain of factor IXa and specific for calcium-dependent conformation, and mAb 3A6 against the heavy chain of factor IXa, were prepared (23, 24). A monoclonal antibody, ESH8, against the C2 domain of factor VIII and recognizing residues 2248–2285 (4, 5) was purchased from American Diagnostica Inc. (Stamford, CT). A horseradish peroxidase (HRP)-labeled monoclonal antibody was prepared using Peroxidase Labeling Kit-NH_2 (Dojindo Molecular Technologies Inc., Kumamoto, Japan). Human factor IXa, factor X, and EGR-ck (Hematologic Technologies, Inc., Essex Junction, VT), factor Xa (Enzyme Research Laboratories, Inc., South Bend, IN), thrombin (Sigma), recombinant hirudin (Calbiochem), and chromogenic Xa substrate S-2222 (Chromogenix, Milano, Italy) were purchased commercially. Gla domainless (GDless) factor IXa was prepared from factor IXa by limited chymotryptic digestion (25). Briefly, α-chymotrypsin was incubated with factor IXa in a 1:24 ratio (w/w) at 4 °C. The reaction was then quenched using 5 mM diisopropyl fluorophosphate, and the GDless factor IXa was separated from undigested factor IXa and the Gla domain-containing peptide (residues 1–42) using ion exchange chromatography. Molecular mass was estimated by SDS-PAGE. The amidolytic activity of GDless factor IXa was less than 0.2%. Phospholipid vesicles containing 10% phosphatidylserine, 60% phosphatidylcholine, and 30% phosphatidylethanolamine (Sigma) were prepared using *N*-octyl glucoside (26). Synthetic peptides consisting of overlapping sequences of 13 residues encompassing 2182–2249 within the factor VIII C2 domain were prepared by Biosynthesis (Lewisville, TX). They were purified by reverse phase HPLC (purity >95%) and were confirmed by mass spectrometry analysis.

Construction, Expression, and Purification of Factor VIII rC2—The rC2 was prepared using the protocol described by Takeshima *et al.* (27). Briefly, cDNA encoding the C2 domain of human factor VIII with a 4-amino acid NH_2-terminal extension (Val^{2169}–Tyr^{2332}) was constructed, transformed, and expressed in *Pichia pastoris* cells. The product was purified using ammonium sulfate fractionation and cation exchange HPLC (TSK-GEL CM-3SW; TOSOH Corp., Tokyo, Japan). SDS-PAGE analysis demonstrated >95% purity. The rC2 protein was identified as a single peak by a gel filtration and had a mass 18,626.6 on LC/MS analysis, closely matching the expected mass of 18,627.3.

Preparation of EGR-GDless Factor IXa—Factor IXa (10 μM) or GDless factor IXa (2.3 μM) was inactivated overnight at 4 °C by the addition of a 20-fold molar excess of EGR-ck in 20 mM HEPES, pH 7.2, 150 mM NaCl, and 0.01% Tween 20 (HBS buffer). Unbound EGR-ck was removed by extensive dialysis at 4 °C in the same buffer. Chromogenic assays demonstrated less than 0.2% residual activity of factor IXa or GDless factor IXa, respectively.

Preparation of rC2 Proteolytic Fragments—The rC2 (16.7 μM) was digested for 96 h at 37 °C with *Staphylococcus aureus* V8 protease (5.4 μM; Wako Pure Chemical Industries Ltd., Osaka, Japan) in 100 mM Tris-Tricine, pH 8.4, 150 mM NaCl, and 0.1% SDS. The digest was treated with the SDS-Out™ precipitation kit (Pierce) to remove the SDS and was fractionated by reverse phase HPLC using TSKgel ODS-100Z (5 μm; Tosoh Corp.). The reaction mixture was loaded onto a column equilibrated with 90% distilled H_2O, 10% acetonitrile in 0.1% trifluoroacetic acid and eluted with a linear gradient of 10–50% acetonitrile over 60 min. Fragments were detected at 216 nm and automatically collected in 500-μl aliquots and lyophilized. The fragments exhibited excellent solubility following their resuspension in HBS buffer. Protein concentrations were determined by the method of Bradford (28). Electrophoresis of the purified fragments followed by staining with GelCode Blue Stain Reagent (Pierce) showed >95% purity.

ELISA-based Binding Assay—Microtiter wells were coated with 200 nM rC2 (100 μl) in 100 mM sodium bicarbonate, pH 9.6, overnight at 4 °C. The wells were washed with HBS buffer and were blocked with the same buffer containing 5% BSA for 2 h at 37 °C. EGR-factor IXa or EGR-GDless factor IXa was then added and incubated in HBS buffer containing 1 mM $CaCl_2$ and 5% BSA for 2 h at 37 °C. Bound EGR-factor IXa was quantified by the addition of HRP-labeled anti-factor IXa mAb 3A6 and *o*-phenylenediamine dihydrochloride substrate. Reactions were quenched by the addition of 2 M H_2SO_4, and absorbances were measured at 492 nm using a Labsystems Multiskan Multisoft microplate reader (Labsystems, Helsinki, Finland). Control experiments demonstrated that mAb 3A6 did not affect the reaction between factor VIII and factor IXa (data not shown). The amount of nonspecific binding of HRP-labeled IgG in the absence of factor VIII was <5% of the total signal. Specific binding was recorded after subtracting the nonspecific binding. In competitive inhibition assays, the competitor proteins were incubated with 100 nM EGR-factor IXa for 2 h at 37 °C prior to the addition to immobilized rC2. The percentage of inhibition was calculated using the equation, (bound absorbance − non-

specific absorbance)/(maximum − nonspecific) × 100 (%). Absorbance in the absence of competitive protein or immobilized rC2 was regarded as maximum or nonspecific, respectively.

SPR-based Binding Assay—The kinetics of rC2 and EGR-factor IXa interaction were determined in SPR-based assays using a Biacore X instrument (BIAcore AB, Uppsala, Sweden). EGR-factor IXa was covalently coupled to the surface of a CM5 chip at a coupling density of ~7 ng/mm^2. Binding (association) of the ligand was monitored in 10 mM HEPES, pH 7.4, 150 mM NaCl, 1 mM $CaCl_2$, and 0.005% surfactant P20, at a flow rate of 20 μl/min for 2 min at 37 °C. The dissociation of bound ligand was monitored for a 2-min period by replacing the ligand-containing buffer with buffer alone. The level of nonspecific binding corresponding to ligand binding to the uncoated chip was subtracted from the signal. The rate constants for association (k_a) and dissociation (k_d) were determined by nonlinear regression analysis (29, 30) using the evaluation software provided by Biacore AB. Equilibrium dissociation constants (K_d) were calculated as k_d/k_a.

Factor Xa Generation Assays—The rate of conversion of factor X to factor Xa was monitored in a purified system (18, 31). Factor Xa was generated at 22 °C in HBS buffer containing 1 mM $CaCl_2$ and 0.1% BSA. For assays in the absence of phospholipid, 200 nM factor VIII was activated by 10 nM thrombin. Thrombin activity was inhibited after 1 min by the addition of 2.5 units/ml hirudin, and factor Xa generation was initiated by the addition of 5 nM factor IXa and 1 μM factor X. Experiments in the absence of factor VIIIa were performed under the same conditions except for 20 nM factor IXa. For assays in the presence of phospholipid, 30 nM factor VIII was activated by 10 nM thrombin in the presence of 20 μM phospholipid. Thrombin activity was inhibited after 1 min by hirudin, and factor Xa generation was initiated by the addition of 0.5 nM factor IXa and the indicated amounts of factor X. Aliquots were removed at appropriate times to assess initial rates of product formation and added to tubes containing EDTA (100 mM final concentration) to stop the reaction. Rates of factor Xa generation were determined at 405 nm using a microtiter plate reader after the addition of chromogenic substrate, S-2222 (0.46 mM final concentration). Factor Xa generation was quantified by extrapolation from a standard curve prepared using known amounts of factor Xa.

ELISA for Factor VIII or EGR-factor IXa Binding to Phosphatidylserine—ELISA were performed using a minor modification of a previously reported method (7). Briefly, 50 μM 1,2-dioleoyl-*sn*-glycero-3-phospho-L-serine (Sigma) in methanol was immobilized onto each well of a microtiter plate and allowed to air dry at 4 °C overnight. After washing with HBS buffer, the wells were blocked for 2 h at 37 °C with HBS buffer containing 5% BSA. Factor VIII or EGR-factor IXa was added to each well in HBS buffer containing 1 mM $CaCl_2$ and 5% BSA and incubated for 2 h at 37 °C. Bound factor VIII was detected using anti-factor VIII mAb ESH8, followed by HRP-labeled anti-mouse second antibody. Bound EGR-factor IXa was detected using HRP-labeled mAb 3A6.

NH_2-terminal Sequence Analysis—The C2 fragments were blotted onto polyvinylidene difluoride membranes, stained with Gelcode Blue, and excised. NH_2-terminal sequence analyses of the purified fragments were performed using an Applied Biosystems model 491 sequencer (Foster City, CA). Samples were subjected to 5 or 7 cycles of automated sequencing.

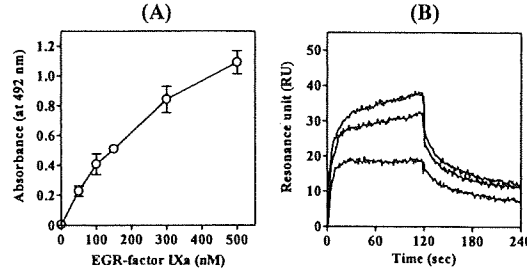

FIGURE 1. **Direct binding of EGR-factor IXa to rC2.** *A*, ELISA-based assay. Various concentrations of EGR-factor IXa were reacted with rC2 (200 nM) that had been immobilized onto microtiter wells for 2 h at 37 °C, as described under "Materials and Methods." Bound EGR-factor IXa was detected using HRP-labeled anti-factor IXa mAb 3A6. Absorbance values were plotted as a function of the concentration of EGR-factor IXa. Experiments were performed at least three separate times, and average ± S.D. values are shown. *B*, SPR-based assay. Various concentrations of rC2 were injected onto the EGR-factor IXa (~7 ng/mm^2) immobilized onto the sensor chip at a flow rate of 20 μl/min for 2 min, followed by a change of running buffer for 2 min as described under "Materials and Methods." The *three lines* illustrate representative response curves for the different concentrations of rC2 (100, 300, and 500 nM, respectively). Experiments were performed at least three separate times.

Solvent-accessible Surface Area Analysis—The solvent accessibilities at the interface for the residues 2182–2259 of the C2 domain were calculated from the atomic coordinates using Marc Gerstein's calc-surface program (32) available from the Helix Systems Web site. The atomic coordinates of human factor VIII and C2 domain were retrieved from the Protein Data Bank (code 2R7E and 1D7P, respectively). Values that are more positive represent a greater probability of surface exposure.

RESULTS

Binding of EGR-factor IXa to the C2 Domain—Blostein *et al.* (21) have recently reported that the Gla domain of factor IXa interacts with the light chain of factor VIIIa. The C2 domain of factor VIIIa and the Gla domain of factor IXa are involved in phospholipid-binding, and we surmised, therefore, that they could be juxtaposed in the factor Xase complex and that the C2 domain might associate directly with the Gla domain of factor IXa. To investigate this hypothesis, we initially examined the direct binding of factor IXa to immobilized rC2 using microtiter-based, solid phase binding assays. An active site-modified EGR-factor IXa preparation was used in these experiments to eliminate difficulties of interpretation in the presence of enzymatically active factor IXa. Various concentrations of EGR-factor IXa were incubated with immobilized rC2 (200 nM). Bound EGR-factor IXa was detected using anti-factor IXa mAb 3A6, recognizing the heavy chain of its protease. EGR-factor IXa bound to immobilized rC2 in a dose-dependent manner (Fig. 1*A*). Control experiments using an anti-C2 mAb demonstrated that immobilized rC2 was not affected by the ionic strength of the wash buffer or the duration of the wash and incubation steps subsequent to C2 binding (data not shown). To confirm the specificity of this binding, various concentrations of factor VIII or rC2 were preincubated with EGR-factor IXa (100 nM) in

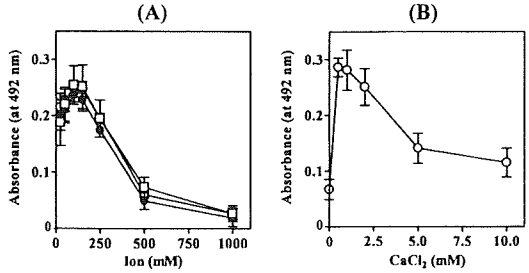

FIGURE 2. **Effect of ionic strength on EGR-factor IXa and rC2 interaction.** *A*, NaCl, KCl, and LiCl effect. EGR-factor IXa (100 nM) was incubated with immobilized rC2 (200 nM) in HBS buffer containing 1 mM $CaCl_2$, 5% BSA, and various amounts of NaCl (*open circles*), KCl (*closed circles*), and LiCl (*open squares*) in an ELISA-based assay. *B*, $CaCl_2$ effect. EGR-factor IXa was incubated with immobilized rC2 in HBS buffer containing 5% BSA and various amounts of $CaCl_2$. EGR-factor IXa bound in the absence of $CaCl_2$ refers to an experiment in the presence of 10 mM EDTA. Experiments were performed at least three separate times, and average ± S.D. values are shown.

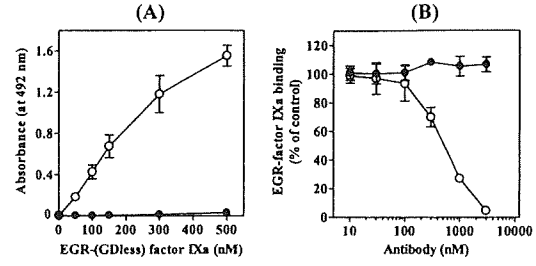

FIGURE 3. **Contribution of the Gla domain of EGR-factor IXa for rC2 interaction.** *A*, various concentrations of EGR-factor IXa (*open circles*) or EGR-GDless factor IXa (*closed circles*) were incubated with immobilized rC2 (200 nM) for 2 h at 37 °C in an ELISA-based assay. *B*, EGR-factor IXa (100 nM) was preincubated with various concentrations of mAb IXa-GD IgG (*open circles*) or normal murine IgG (*closed circles*) for 2 h at 37 °C, prior to incubation with immobilized rC2. Absorbance values for the EGR-factor IXa binding to rC2 in the absence of competitor represent the 100% level. The percentage of EGR-factor IXa binding was plotted as a function of antibody concentration. Experiments were performed at least three separate times, and average ± S.D. values are shown.

the fluid phase prior to addition to the immobilized rC2. Factor VIII and rC2 inhibited EGR-factor IXa binding to immobilized rC2 by ~90 and ~60%, respectively (data not shown), confirming specificity of the assay.

We further evaluated interactions by an alternative approach using real time SPR-based assays. This technique provides information on kinetic and equilibrium binding constants (29, 30). A range of concentrations of rC2 were added to EGR-factor IXa immobilized onto a sensor chip. Fig. 1*B* shows representative curves corresponding to the association/dissociation of rC2. The data could be comparatively well fitted by nonlinear regression using a 1:1 binding model with drifting base line. Kinetic constants showed that rC2 bound to EGR-factor IXa with mild affinity (K_d = 108 ± 27 nM, k_d/k_a = 2.45 × 10^{-2} s^{-1}/2.36 × 10^5 M^{-1} s^{-1}). In ELISA-based assays, the apparent K_d value appeared to be higher (~400 nM), compared with that obtained by SPR-based assays. Since ELISA is not an equilibrium binding assay, the multiple steps of incubation and wash may affect the detection for lower concentrations of EGR-FIXa. The results indicated that the C2 domain of factor VIII interacted directly with factor IXa.

Characterization of the Interaction between the C2 Domain and EGR-factor IXa—The light chain of factor VIIIa interacts with factor IXa in electrostatic and calcium-dependent mechanisms (19). To further characterize this interaction, factor IXa (100 nM) was mixed with various amounts of NaCl and incubated with immobilized rC2. Control experiments showed that the amount of immobilized rC2 or the reactivity of antibody was not affected even at a higher concentration of NaCl (data not shown). Binding of EGR-factor IXa to rC2 was maximal at physiological concentrations of NaCl (~150 mM; Fig. 2*A*). Higher concentrations of NaCl incrementally weakened this interaction, however, and consequently binding was significantly decreased by ~95% at elevated ionic strengths, supporting the salt sensitivity of this interaction. The Na^+-bound factor IXa drastically enhances catalytic activity toward factor X and increases the affinity for factor VIIIa (33, 34). However, other monovalent cations, K^+ and Li^+, also inhibited this binding similarly, suggesting that this effect was not due to a specific interaction of Na^+-factor IXa.

Ca^{2+} is known to be required for the structural and functional integrity of factor IXa, and hence the effect of Ca^{2+} on factor IXa-rC2 interaction was also examined in the current experiments. Binding of factor IXa to immobilized rC2 was investigated in buffer containing various amounts of $CaCl_2$. EDTA (10 mM) was added to the reaction mixtures to assess binding in the absence of Ca^{2+}. The presence of Ca^{2+} up to ~1.0 mM markedly increased factor IXa binding by ~6-fold compared with that in the absence of Ca^{2+} (Fig. 2*B*). Optimal binding was observed at approximately physiological concentrations of free Ca^{2+} (~1.3 mM). Binding was significantly inhibited by increments of Ca^{2+} >1 mM. The data were consistent, therefore, with a role for Ca^{2+} in C2-factor IXa interaction, although it was not possible to distinguish between a direct or indirect role for Ca^{2+} in mediating this effect.

Binding of the Gla Domain of Factor IXa to the C2 Domain—To investigate whether the Gla domain of factor IXa participates in direct interactions with the C2 domain of factor VIII, EGR-GDless factor IXa was prepared by chymotrypsin digestion and EGR-ck labeling, as described under "Materials and Methods." Control experiments demonstrated that EGR-GDless factor IXa and EGR-factor IXa were similarly reactive with anti-factor IXa mAb 3A6 in the ELISA (data not shown). The binding of EGR-GDless factor IXa to immobilized rC2 was markedly lower than that of EGR-factor IXa even at the maximum concentration employed (500 nM; Fig. 3*A*). SPR-based assays also showed that rC2 failed to react with EGR-GDless factor IXa (data not shown). In addition, competitive experiments using an anti-factor IXa mAb, mAb IXa-GD, recognizing the Gla domain of factor IXa and dependent on the presence of Ca^{2+}, demonstrated that the monoclonal antibody blocked binding of EGR-factor IXa to rC2 (up to ~95%) in a dose-dependent manner (IC_{50}; 758 ± 93 nM) (Fig. 3*B*). These findings were in keeping with a significant role for the Gla domain of factor IXa in direct binding to the C2 domain of factor VIII.

To assess the functional role of the interaction between the C2 domain and Gla domain of factor IXa in the factor Xase complex, we examined the effect of rC2 or mAb IXa-GD on factor VIIIa/factor IXa-mediated activation of factor X in an

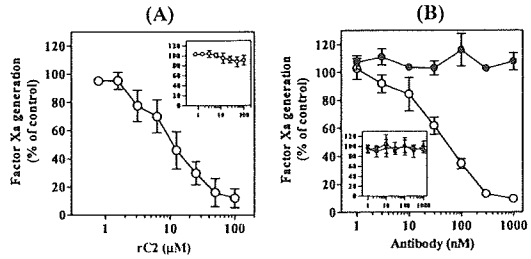

FIGURE 4. **Inhibition of rC2 and mAb IXa-GD in factor VIIIa/factor IXa-mediated factor X activation in the absence of phospholipid.** Various concentrations of rC2 (*open circles*) (*A*) or mAb IXa-GD (*open circles*) (*B*) or normal murine IgG (*closed circles*) were preincubated with 5 nM factor IXa for 2 h at 37 °C. Factor Xa generation was initiated by the addition of thrombin-activated factor VIIIa (200 nM) and 1 μM factor X under the conditions described under "Materials and Methods." The initial rate of factor Xa generated in the absence of competitor represents the 100% level and was 1.19 ± 0.14 nM/min. Initial rates of factor Xa generation were plotted as a function of rC2 or antibody concentration. The *inset* shows the experiments in the absence of factor VIIIa under similar conditions except for 20 nM factor IXa. The initial rate of factor Xa generated in the absence of competitor (100% level) was 0.0034 ± 0.0001 nM/min. Experiments were performed at least three separate times, and average ± S.D. values are shown.

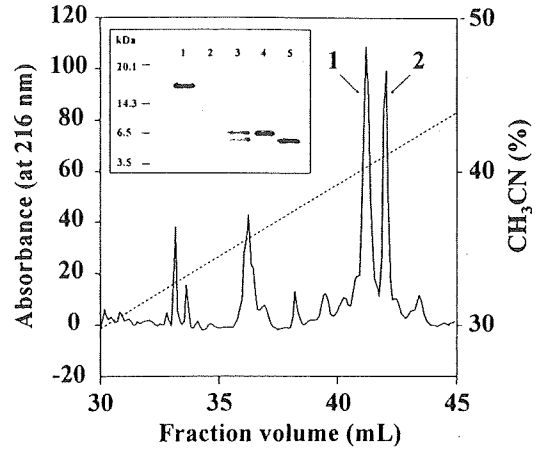

FIGURE 5. **Reverse phase HPLC and SDS-PAGE of V8 protease-cleaved rC2.** *S. aureus* V8 protease-cleaved C2 fragments were fractionated by reverse phase HPLC. The *broken line* represents acetonitrile concentration (10–50%), and fragments were detected at 216 nm (*solid line*). The *inset* shows that the proteins were analyzed by SDS-PAGE using 16.5% peptide gel under nonreducing conditions, followed by staining with GelCode Blue. *Lane 1*, 1.5 μg of rC2; *lane 2*, 0.75 μg of V8 protease; *lane 3*, 1.5 μg of rC2 digested with 0.75 μg of V8 protease; *lane 4*, 0.5 μg of fragment in peak fraction 1; *lane 5*, 0.5 μg of fragment in peak fraction 2. The positions of molecular mass markers in kDa are indicated to the *left*.

amidolytic assay. For this assay, 200 nM factor VIII was activated by thrombin and incubated with mixtures of 5 nM factor IXa and various concentrations of rC2 or mAb IXa-GD. Factor Xa generation was initiated by the addition of 1 μM factor X. The rC2 competes with factor VIII for binding to phospholipid membranes, and for this reason, the assays were performed in the absence of phospholipid. The addition of rC2 and mAb IXa-GD markedly decreased the rates of factor Xa generation (by >90%) in a dose-dependent manner, with the IC_{50} values of 10.9 ± 3.8 μM and 43.2 ± 15.3 nM, respectively (Fig. 4, *A* and *B*). To exclude the possibility that rC2 and mAb IXa-GD directly affected factor IXa-catalyzed activation of factor X, factor Xa generation was further examined in the absence of factor VIIIa. As expected, there was little inhibition of factor Xa generation in the presence of rC2 or mAb IXa-GD (Fig. 4, *inset*), confirming that the reactions were governed by factor VIIIa. The results indicated that association between the C2 domain of factor VIII and the Gla domain of factor IXa played a significant role in the assembly of the factor Xase complex and hence factor IXa-catalyzed activation of factor X in the presence of factor VIIIa.

Purification and Characterization of rC2-digested Fragments—To localize factor IXa-interactive regions within the C2 domain, limited *Staphylococcus aureus* V8 protease digests of rC2 were prepared. SDS-PAGE analysis demonstrated the presence of two large fragments of apparent mass 7.5- and 6.2-kDa that were significantly smaller than the initial rC2 (~16 kDa) (Fig. 5*B*). The digestion of rC2 by V8 protease required denaturing conditions with 0.1% SDS, and we confirmed that the binding of SDS-treated, uncleaved rC2 to EGR-factor IXa was similar to that of the non-SDS-treated product in the ELISA-based assay (data not shown). EGR-factor IXa bound to immobilized, unfractionated V8 protease-cleaved rC2 in a dose-dependent manner (data not shown), prompting us to further isolate and purify the cleaved fragments. The two fragments were not able to be separated by ion exchange HPLC using CM, Mono-Q, and Mono-S under any salt and pH conditions but were resolved by reverse phase HPLC (Fig. 5). SDS-PAGE confirmed that these fractions, designated as peak 1 and peak 2, represented the 7.5- and 6.2-kDa fragments, respectively (Fig. 5, *inset*). Some smaller peaks were observed, but the bands were poorly detectable in SDS-PAGE and appeared to represent further minor degradation of rC2. The peak 1 and peak 2 fractions were further characterized by size exclusion chromatography, and each was shown to elute as a single peak, indicating that the fragments were monomeric in solution (data not shown).

Automated NH_2-terminal sequence analysis identified that the sites of cleavage responsible for the generation of the two C2 fragments were located at residues Glu^{2181}-Ser^{2182} and Glu^{2259}-Phe^{2260} for the ~7.5- and ~6.2-kDa fragments, respectively (Table 1). In addition, LC/MS analysis indicated that the molecular mass of fragment 1 (7.5 kDa) and fragment 2 (6.2 kDa) was 8827.25 ± 5.70 and 7355.63 ± 0.68 Da, respectively. On the basis of the previous molecular masses determined by LC/MS, NH_2-terminal sequence analysis, and specificity of V8 protease cleavage site (-Glu-*X* and/or -Asp-*X*), the deduced protein sequences of the two C2 fragments matched Ser^{2182}–Glu^{2259} (expected mass, 8823.08 Da) and Phe^{2260}–Glu^{2322} (expected mass, 7354.39 Da). Hence, the ~7.5- and ~6.2-kDa C2 fragments were designated as C2-(2182–2259) and C2-(2260–2322), respectively.

Binding of the Isolated C2 Fragments to EGR-factor IXa and the Effects on Factor Xa Generation—To determine whether the C2-(2182–2259) and/or C2-(2260–2322) were able to bind to factor IXa, we investigated direct binding in ELISA-based assays, as described above. EGR-factor IXa bound directly to immobilized C2-(2182–2259) (600 nM) in a dose-dependent manner, although in this instance, the binding efficiency was weaker than that of the uncleaved rC2 (Fig. 6*A*). In contrast, very limited binding of EGR-factor IXa to immobilized

TABLE 1

Amino-terminal sequence analysis of the C2 fragments

Sequences were determined as described under "Materials and Methods" and were aligned using published factor VIII sequences (1, 2).

	Cycle number						
	1	2	3	4	5	6	7
Residues 2182–2188	Ser	Lys	Ala	Ile	Ser	Asp	Ala
C2 fragment 1	Ser	Lys	Ala	Ile	Ser	Asp	Ala
pmol	10.4	17.7	14.4	14.3	8.4	6.6	7.9
Residues 2260–2264	Phe	Leu	Ile	Ser	Ser		
C2 fragment 2	Phe	Leu	Ile	Ser	Ser		
pmol	10.7	10.3	11.0	5.5	5.4		

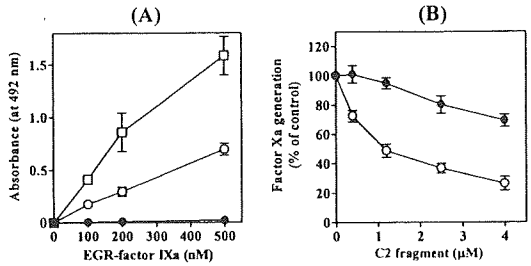

FIGURE 6. **Binding of EGR-factor IXa to C2 fragments and the inhibitory effects on factor Xa generation.** A, binding of EGR-factor IXa. Various concentrations of EGR-factor IXa were incubated with immobilized C2-(2182–2259) (600 nM; *open circles*), C2-(2260–2322) (600 nM; *closed circles*), and intact rC2 (100 nM; *open squares*) for 2 h at 37 °C in an ELISA-based assay. Absorbance values were plotted as a function of the concentration of EGR-factor IXa. *B*, inhibition of factor Xa generation in the absence of phospholipid. Various amounts of C2-(2182–2259) (*open circles*) or C2-(2260–2322) (*closed circles*) were preincubated with 5 nM factor IXa for 2 h at 37 °C, and factor Xa generation was initiated with the addition of thrombin-activated factor VIIIa (200 nM) and 1 μM factor X. The initial rate of factor Xa generated in the absence of competitor (100% level) was 1.46 ± 0.19 nM/min. Initial rates of factor Xa generation were plotted as a function of C2 fragment concentration. Experiments were performed at least three separate times, and average ± S.D. values are shown.

C2-(2260–2322) was observed. In control experiments, EGR-GDless factor IXa did not bind to either immobilized C2 fragment (data not shown). To assess the functional capacity of the two C2 fragments in factor Xase assembly, amidolytic assays were again repeated in the absence of phospholipid. Factor VIII (200 nM) was activated by thrombin and incubated with factor IXa (5 nM)/C2 fragment mixtures and factor X (1 μM). The C2-(2182–2259) competitively inhibited factor Xa generation by ~80% at the maximum concentration employed (IC_{50} = 1.2 μM; Fig. 6*B*). The effect of C2-(2260–2322) was significantly lower than that of C2-(2182–2259), however, and inhibited factor Xa generation by ~30%. Collectively, these data suggest that an interactive site(s) for the Gla domain of factor IXa was likely to be located within residues 2182–2259 of the C2 domain.

Effects of Synthetic C2 Peptides on rC2 and EGR-factor IXa Interaction and on Factor Xa Generation in the Absence of Phospholipids—On the basis of the competitive binding assays and ELISA, we focused on the 2182–2259 region in the C2 domain to further identify the potential factor IXa-interactive site. The C2-factor IXa interaction is electrostatically dependent (see Fig. 2*A*), suggesting that both interactive sites are surface-exposed. The analysis of solvent-accessible surface area was utilized, therefore, to examine regions within residues 2182–2259 exhibiting a high probability of being surface-exposed. The solvent accessibilities at the interface were calculated from atomic coordinates in the structures of factor VIII and C2 (Protein Data Bank code 2R7E and 1D7P, respectively), and they were similar. Using this approach, overlapping synthetic peptides encompassing the 2182–2249 region were prepared (Fig. 7). Since the C2-factor IXa interaction was not affected by anti-C2 mAb ESH8 with epitopes 2248–2285 (data not shown), the 2248–2259 region was excluded. Effects of peptides to block C2-factor IXa interaction and to inhibit factor Xa generation were examined.

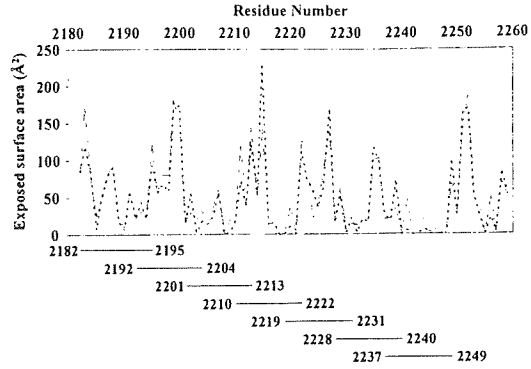

FIGURE 7. **Accessible surface area of residues 2182–2259 of the C2 domain.** The solvent accessibilities at the interface for the residues 2182–2259 of the C2 domain were calculated from the atomic coordinates in the structure of factor VIII (*solid lines*) and C2 (*dashed lines*) using Marc Gerstein's calc-surface program (see "Materials and Methods"). Accessible surface area (Å²) was used to estimate the probability of a segment being exposed to the surface. Synthetic peptides corresponding to regions of high surface probability are indicated by the *horizontal bars* and are identified by residue numbers for the segments.

The synthetic peptide corresponding to residues 2228–2240 (designated peptide 2228–2240) inhibited binding of EGR-factor IXa to rC2 by ~75% at the maximum concentrations employed (at 1 mM) (Fig. 8*A*). The IC_{50} value was ~400 μM. The other six peptides, corresponding to residues 2182–2195, 2192–2204, 2201–2213, 2210–2222, 2219–2231, and 2237–2249, demonstrated no inhibitory effects. Moreover, a control peptide (VKMTKQFDVQLWE), comprising the 2228–2240 residues in a random sequence, completely lost the ability to inhibit this interaction (data not shown). The inhibitory effects of these peptides were further studied in the factor Xa generation assay. The peptide 2228–2240, which blocked C2-factor IXa interaction, depressed factor Xa generation by ~75% at the maximum concentration employed (IC_{50} ~ 25 μM) (Fig. 8*B*). The other C2 peptides and the scrambled peptide had little effect. The ability of peptide 2228–2240 to inhibit factor Xa generation appeared to be more significant than that in the binding assay. It seemed likely, therefore, that peptide 2228–2240 not only affected interactions between the Gla domain of factor IXa and the C2 domain but also allosterically modulated other reactions. Nevertheless, the findings suggest that interactive site for the Gla domain of factor IXa was located within residues 2228–2240 of the C2 domain.

Effects of peptide 2228–2240 on Factor Xa Generation in the Presence of Phospholipid—Intact C2 and isolated C2 fragments contain phospholipid-binding regions, and to preclude interference by these reactions, our current factor Xa generation

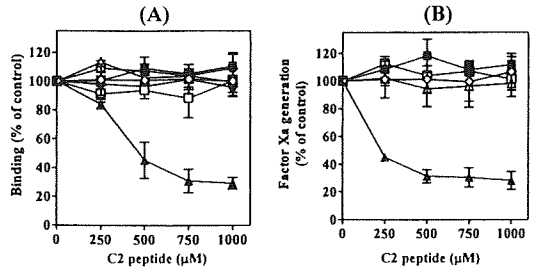

FIGURE 8. **Inhibition of synthetic C2 peptides on EGR-factor IXa binding to rC2 and on factor Xa generation in the absence of phospholipid.** *A*, EGR-factor IXa binding to rC2. Various amounts of synthetic C2 peptide were preincubated with 100 nM EGR-factor IXa for 2 h at 37 °C, prior to the addition to immobilized rC2 (200 nM) in an ELISA-based assay. Absorbance values for the EGR-factor IXa binding to rC2 in the absence of competitor represent the 100% level. The percentage of EGR-factor IXa binding was plotted as a function of peptide concentration. *B*, factor Xa generation in the absence of phospholipid. Various amounts of C2 peptide were preincubated with 5 nM factor IXa for 2 h at 37 °C, and factor Xa generation was initiated with the addition of thrombin-activated factor VIIIa (200 nM) and 1 μM factor X. The initial rate of factor Xa generated in the absence of competitor (100% level) was 0.83 ± 0.01 nM/min. Initial rates of factor Xa generation were plotted as a function of C2 peptide concentration. *Open circles*, peptide 2182–2195; *closed circles*, peptide 2192–2204; *open squares*, peptide 2201–2213; *closed squares*, peptide 2210–2222; *open triangles*, peptide 2219–2231; *closed triangles*, peptide 2228–2240; *open diamonds*, peptide 2237–2249. Experiments were performed at least three separate times, and average ± S.D. values are shown.

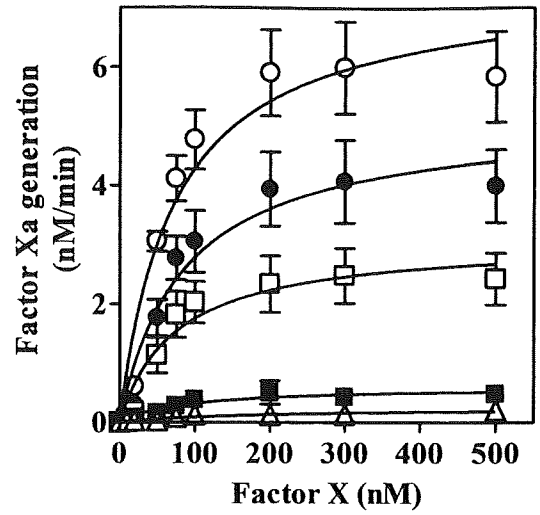

FIGURE 9. **Effect of peptide 2228–2240 on factor Xa generation in the presence of phospholipid.** Factor IXa (0.5 nM) was preincubated with 0 μM (*open circles*), 2.5 μM (*closed circles*), 5 μM (*open squares*), 10 μM (*closed squares*), and 15 μM (*open triangle*) of peptide 2228–2240 for 2 h at 37 °C. Factor Xa generation was initiated by the addition of thrombin-activated factor VIIIa (30 nM) and various concentrations of factor X (0–500 nM) in the presence of phospholipid vesicles (20 μM). Initial rates of factor Xa generation were plotted as a function of factor X concentration and fitted to the Michaelis-Menten equation by nonlinear least squares regression. Experiments were performed at least three separate times, and average ± S.D. values are shown. The V_{max} values in the presence of 0, 2.5, 5, and 10 μM peptide were 7.42 ± 0.85, 5.15 ± 0.73, 3.07 ± 0.49, and 0.61 ± 0.12 nM/min, respectively. The K_m values were 72.9 ± 25.5, 84.8 ± 34.9, 75.0 ± 36.0, and 89.6 ± 51.3 nM, respectively. The kinetic parameters in the presence of 15 μM peptide could not be determined because of very low values.

assays were performed in the absence of phospholipid. Crystal structure analysis has demonstrated that binding of the C2 domain to phospholipid membranes involves three hydrophobic "feet" containing residues Met^{2199}/Phe^{2200}, Val^{2223}, and Leu^{2251}/Leu^{2252} and four basic residues, Arg^{2215}, Arg^{2220}, Lys^{2227}, and Lys^{2249} (35, 36). The factor IXa-interactive site that we have identified within residues 2228–2240 appears, therefore, to be in close proximity to, but not likely to be overlapping, the phospholipid-binding region. In support of this contention, we found that binding of factor VIII and factor IXa to phosphatidylserine was not significantly inhibited by peptide 2228–2240 (data not shown). Nevertheless, to further examine the physiological role of peptide 2228–2240 binding to the Gla domain of factor IXa, factor Xa generation was measured in the presence of factor VIIIa and phospholipid. Factor VIII (30 nM) was activated by thrombin and incubated with factor IXa (0.5 nM)/peptide 2228–2240 mixtures together with various concentrations of factor X in the presence of phospholipid (20 μM). Since rC2-factor IXa interaction was optimal at relatively low concentrations of Ca^{2+} (~1 mM), under these circumstances, the V_{max} was ~20-fold lower than that previously reported (31). Nevertheless, in the presence of peptide 2228–2240, the K_m value remained unchanged, whereas the V_{max} was decreased, dependent on the concentration of the peptide (Fig. 9). Factor Xa generation was completely inhibited (>95%) in the presence of 15 μM peptide. These results suggested that peptide 2228–2240 inhibited factor Xa generation on phospholipid micelles by noncompetitive inhibitory mechanisms. Furthermore, peptide 2228–2240 did not affect factor Xa generation using GDless factor IXa in place of factor IXa in these assays (data not shown), again indicating that peptide 2228–2240 specifically bound to the Gla domain of factor IXa but did not moderate interactions between factor VIIIa and factor X.

DISCUSSION

The enzyme factor IXa and its cofactor factor VIIIa are assembled on phospholipid membranes for the activation of factor X. In previous reports, factor IXa recognition sites were identified within the A2 and A3 domains of factor VIIIa. In the A2 domain, the extended surface, centered on residues 484–509 (16), 558–565 (17), and 708–717 (18), appeared to interact with the factor IXa with weak affinity (~300 nM) (15). In contrast, in the A3 domain, the light chain, including residues 1804–1818 (20), interacted with the protease with high affinity (~15 nM) (19). The structural model of factor VIIIa-factor IXa on phospholipid membranes reported by Blostein *et al.* (21) proposed that the C2 domain of factor VIIIa and the Gla domain of factor IXa bound to phospholipid would be in close proximity, suggesting that both domains might bind to each other. In the present study, we show for the first time that the residues 2228–2240 in the C2 domain and the Gla domain of factor IXa bind to each other.

This conclusion is based on several novel findings using the established models. (i) Direct binding studies demonstrated that active site-modified EGR-factor IXa bound to the C2 domain with mild affinity (~100 nM), whereas GDless EGR-factor IXa failed to bind. In addition, mAb IXa-GD, recognizing the Gla domain of factor IXa, blocked C2-factor IXa interaction. (ii) A factor Xa generation assay without phospholipid showed that rC2 and mAb IXa-GD inhibited factor IXa-medi-

ated factor X activation in the presence of factor VIIIa. (iii) A C2-(2182–2259) fragment, derived from V8 protease-cleaved rC2, directly bound to EGR-factor IXa and inhibited factor Xa generation, whereas the C2-(2260–2322) did not bind. (iv) Competitive assays, using overlapping synthetic peptides encompassing residues 2182–2259, showed that peptide 2228–2240 significantly inhibited both factor IXa binding and factor Xa generation, independently of phospholipid. These data identified amino acid residues 2228–2240 within the C2 domain as essential for factor IXa docking.

In the present study, we utilized EGR-factor IXa, a catalytically inactive derivative of factor IXa, in direct binding experiments. Modified factor IXa prepared with EGR-ck is well known to minimize enzyme-catalyzed degradation, but conformational changes and/or steric hindrance due to incorporation of EGR-ck into the active site of factor IXa may cause difficulties. Nevertheless, Lenting *et al.* (19) reported that thrombin-cleaved factor VIII light chain bound to modified factor IXa with high affinity (~15 nM), and we also analyzed direct binding of the C2 domain using untreated factor IXa and EGR-factor IXa. Binding patterns were similar using active factor IXa and EGR-factor IXa (data not shown), suggesting that any potential effects of conformational changes and/or steric hindrance induced by EGR-ck were minimal. The results also indicated that the C2 domain does not participate in docking to the active site pocket of factor IXa.

We obtained direct evidence for a restricted factor IXa-interactive site in the C2 domain using solvent-accessible surface area analysis with overlapping peptides encompassing residues 2182–2259. The sequence 2228–2240 appeared to be specific for this interaction, and a scrambled peptide confirmed this specificity. The peptide 2228–2240 did not affect factor VIII binding to phospholipid, however, in keeping with an earlier study using similar C2 peptides (7). Our observations add significantly to understanding the nature of the factor Xase complex involving factor IXa and the C2 domain of factor VIII. Our suggestion that this region is not related to phospholipid binding by experiments using peptide can be supported by the following reasons.

First, based on the ability of synthetic peptides encompassing residues 2303–2332 in C2 to inhibit factor VIII-phospholipid binding, a major site was previously located within this region (7). In addition, earlier elegant examination of the 1.5 Å x-ray structure of the C2 domain revealed the presence of three hydrophobic "feet" (Met^{2199}/Phe^{2200}, Val^{2223}, and Leu^{2251}/Leu^{2252}) that penetrate the membrane and four basic residues (Arg^{2215}, Arg^{2220}, Lys^{2227}, and Lys^{2249}) that lie underneath the "feet" and stabilize binding by electrostatic interaction with phospholipid (35, 36). These findings show that the 2228–2240 region in C2 is in close proximity to, but is not likely to overlap, the phospholipid-binding region. Second, The interaction between factor IXa and thrombin-cleaved factor VIII light chain, lacking the acidic region of the A3 domain involved in high affinity VWF binding, was not affected by the presence of VWF (19). Our present study also showed that the C2-factor IXa interaction was not affected by VWF (data not shown). Since the C2 domain is involved in VWF binding at a site that overlaps the phospholipid-binding site (8, 9), the 2228–2240 region does not overlap this site. Last, factor VIIIa contacts with residue Phe^{25} and/or Val^{46} of the Gla domain of factor IXa but not with the membrane-binding ω loop (residues 1–11) (21). Furthermore, a naturally occurring mutation (G12R) within the Gla domain is associated with reduced activity of the factor Xase complex but does not affect phospholipid binding (37). These results are consistent with the view that interaction between the Gla domain and the C2 domain is not dependent on phospholipid binding. Taken together, our findings imply that interactions between both domains facilitate a tight ternary complex with phospholipid.

Binding of C2 to the Gla domain of factor IXa was governed by electrostatic and/or calcium-dependent interactions. This mechanism was similar to that observed between the light chain of factor VIII and factor IXa (19). Furthermore, peptide 2228–2240 significantly inhibited (>95%) factor Xa generation in the presence of phospholipid through noncompetitive inhibitory mechanisms, similar to those observed using peptide 1804–1818, previously reported as a factor IXa-binding site in A3. These data strongly indicated that the properties of both interactions were common and that both peptides inhibited the enzyme activity of factor IXa by binding at a site distinct from the substrate binding pocket. Of interest, the binding affinity of C2 for factor IXa (~100 nM) was ~7-fold lower than that of the light chain (~15 nM). In the absence of phospholipid, the inhibitory effect of peptide 2228–2240 on C2-factor IXa interaction was not significantly different from that of peptide 1804–1818 on light chain-factor IXa interaction. In the presence of phospholipid, however, peptide 2228–2240 appeared to inhibit factor Xa generation more strongly than peptide 1804–1818 (IC_{50} ~ 5 and ~600 μM, respectively). The binding affinity of the A3 domain for factor IXa is not known; nevertheless, the high affinity of the light chain appears to make an essential contribution to reactions involving not only the A3 domain but also the C2 domain. Furthermore, the data indicate that peptide 2228–2240 predominantly participates in factor IXa docking for catalyzing the activity of the factor Xase enzyme.

Recently, two groups have reported the intermediate resolution x-ray crystallographic structure of B-domainless factor VIII (38, 39). Factor IXa-interactive sites within factor VIII based on crystal structure reveal that residues 558–565 and 708–717 in A2 and 1804–1818 in A3 are located on one face of factor VIII, whereas residues 484–509 in A2 and our identified 2228–2240 in C2 are located on another face. Ngo *et al.* (39) have constructed a model of the factor VIIIa-factor IXa complex with x-ray crystal structure of human factor VIII and porcine factor IXa backbone with the following constraints. Residues 558–565, 708–717, and 1804–1818 of factor VIIIa interact with the residues 330–339, residues 301–303, and the putative binding region, including EGF domains (Tyr^{69} and Asn^{92}) and Gla domain (Phe^{25}) of factor IXa, respectively. Although this differed from our data in the binding site of C2 for the Gla domain, a factor IXa-interactive site comprising residues 2228–2240 in C2 is unlikely to contact the Gla domain simultaneously according to this model. This discrepancy may be due to conformational change of the C2 domain. Conformational changes in C2 of factor VIIIa upon removal of the NH_2 terminus of the light chain (residues 1649–1689) (40) probably

leads to enhancement of the factor VIIIa affinity for phospholipid membrane (41). This may affect the Gla domain binding. In addition, the C2 domain is relatively loosely docked to the remainder of factor VIII molecules (38, 39); consequently, the position of this domain within active form factor VIIIa on the phospholipid surface may change easily. These findings can be supported by the case of residues 484–509 in A2. The model proposed by Ngo showed that this region did not interact with factor IXa despite the factor IXa-interactive site. Bajaj *et al.* (42) also demonstrated that residues 484–509 in A2 were not in close proximity to one face consisting of residues 558–565, 708–717, and 1804–1818 and did not contact factor IXa. Furthermore, Stoilova-McPhie *et al.* (43) found that it was unable to modify the factor VIII-factor IXa binding model, including the 484–509 region. The following possibilities are raised for this reason: the conformational change in A2 upon binding of the catalytic domain of factor IXa and different A2 arrangement between unactive form factor VIII and active form factor VIIIa. Therefore, it is not so surprising that the 2228–2240 region in factor VIIIa interacts with factor IXa Gla domain.

An earlier report by Nogami *et al.* (11) demonstrated that residues 2253–2270 within the C2 domain of factor VIII contribute to a unique factor Xa-interactive site within the light chain that promotes factor Xa docking during cofactor activation and cleavage of the light chain at Arg^{1689}. Binding of factor Xa to the C2 domain was independent of binding to phospholipid or VWF, indicative of a distinct factor Xa-binding site in the C2 domain. This binding was remarkably similar to that of the C2-factor IXa interaction observed in this study. In addition, interaction between the light chain of factor VIIIa and factor IXa was not inhibited by active site-modified factor Xa (19). However, the C2-factor IXa interaction was not inhibited by anti-C2 mAb ESH8 (data not shown), which recognizes residues 2248–2285 and inhibits the factor VIII-factor Xa interaction (11). These findings suggest that the factor IXa-interactive site in the C2 domain does not overlap the factor VIII-Xa interactive site.

Comparisons of amino acid sequences among human, porcine, murine, and canine factor VIII molecules indicate that residues 2228–2240 within the C2 domain are well conserved, in keeping with the suggestion that this region could be fundamental for interaction with the Gla domain of factor IXa (44–46). This region appears to be unique, and the specific sequence of residues is distinct from those of the factor IXa-interactive sites within the A2 and A3 domains of factor VIIIa (16–18, 20). Naturally occurring mutations of residues 2228–2240 (W2229C, W2229S, Q2231H, V2232A/E, and M2238V) have been reported in the hemophilia A data base (HAMSTeRS), and are seen in mild/moderate hemophilia A. It is tempting to speculate that the pathogenic mechanism for these point mutations might be associated with dysfunctional blood coagulation by moderating interactions between the C2 domain of factor VIIIa and the Gla domain of factor IXa. Furthermore, substitutions at Trp^{2229} to Cys and Val^{2232} to Ala are related to the development of inhibitors (47, 48), consistent with our suggestion that the 2228–2240 region in C2 is surface-exposed and influences antigenicity.

In conclusion, we provide the first evidence for an essential role of the association between the 2228–2240 region of the C2 domain and the Gla domain of factor IXa in the factor Xase complex. Further studies using site-directed mutagenesis are warranted to further clarify the functional role of residues 2228–2240 in the C2 domain.

Acknowledgment—We thank Dr. J. C. Giddings for helpful suggestions.

REFERENCES

1. Toole, J. J., Knopf, J. L., Wozney, J. M., Sultzman, L. A., Buecker, J. L., Pittman, D. D., Kaufman, R. J., Brown, E., Shoemaker, C., Orr, E. C., Amphlett, G. W., Foster, W. B., Coe, M. L., Knudson, G. J., Fass, D. N., and Hewick, R. M. (1984) *Nature* **312,** 342–347
2. Wood, W. I., Capon, D. J., Simonsen, C. C., Eaton, D. L., Gitschier, J., Keyt, B., Seeburg, P. H., Smith, D. H., Hollingshead, P., Wion, K. L., Delwart, E., Tuddenham, E. G. D., Vehar, G. A., and Lawn, R. M. (1984) *Nature* **312,** 330–337
3. Vehar, G. A., Keyt, B., Eaton, D., Rodriguez, H., O'Brien, D. P., Rotblat, F., Oppermann, H., Keck, R., Wood, W. I., Harkins, R. N., Tuddenham, E. G. D., Lawn, R. M., and Capon, D. J. (1984) *Nature* **312,** 337–342
4. Shima, M., Scandella, D., Yoshioka, A., Nakai, H., Tanaka, I., Kamisue, S., Terada, S., and Fukui, H. (1993) *Thromb. Haemost.* **69,** 240–246
5. Saenko, E. L., Shima, M., Rajalakshmi, K. J., and Scandella, D. (1994) *J. Biol. Chem.* **269,** 11601–11605
6. Shima, M., Nakai, H., Scandella, D., Tanaka, I., Sawamoto, Y., Kamisue, S., Morichika, S., Murakami, T., and Yoshioka, A. (1995) *Br. J. Haematol.* **91,** 714–721
7. Foster, P. A., Fulcher, C. A., Houghten, R. A., and Zimmerman, T. S. (1990) *Blood* **75,** 1999–2004
8. Nogami, K., Shima, M., Nakai, H., Tanaka, I., Suzuki, H., Morichika, S., Shibata, M., Saenko, E. L., Scandella, D., Giddings, J. C., and Yoshioka, A. (1999) *Br. J. Haematol.* **107,** 196–203
9. Nogami, K., Shima, M., Giddings, J. C., Takeyama, M., Tanaka, I., and Yoshioka, A. (2007) *Int. J. Hematol.* **85,** 317–322
10. Nogami, K., Shima, M., Hosokawa, K., Nagata, M., Koide, T., Saenko, E. L., Tanaka, I., Shibata, M., and Yoshioka, A. (2000) *J. Biol. Chem.* **275,** 25774–25780
11. Nogami, K., Shima, M., Hosokawa, K., Suzuki, T., Koide, T., Saenko, E. L., Scandella, D., Shibata, M., Kamisue, S., Tanaka, I., and Yoshioka, A. (1999) *J. Biol. Chem.* **274,** 31000–31007
12. Healey, J. F., Barrow, R. T., Tamim, H. M., Lubin, I. M., Shima, M., Scandella, D., and Lollar, P. (1998) *Blood* **92,** 3701–3709
13. van Dieijen, G., Tans, G., Rosing, J., and Hemker, H. C. (1981) *J. Biol. Chem.* **256,** 3433–3442
14. Schmidt, A. E., and Bajaj, S. P. (2003) *Trends Cardiovasc. Med.* **13,** 39–45
15. Fay, P. J., and Koshibu, K. (1998) *J. Biol. Chem.* **273,** 19049–19054
16. Fay, P. J., and Scandella, D. (1999) *J. Biol. Chem.* **274,** 29826–29830
17. Fay, P. J., Beattie, T., Huggins, C. F., and Regan, L. M. (1994) *J. Biol. Chem.* **269,** 20522–20527
18. Jenkins, P. V., Dill, J. L., Zhou, Q., and Fay, P. J. (2004) *Biochemistry* **43,** 5094–5101
19. Lenting, P. J., Donath, M. J., van Mourik, J. A., and Mertens, K. (1994) *J. Biol. Chem.* **269,** 7150–7155
20. Lenting, P. J., van de Loo, J. W., Donath, M. J., van Mourik, J. A., and Mertens, K. (1996) *J. Biol. Chem.* **271,** 1935–1940
21. Blostein, M. D., Furie, B. C., Rajotte, I., and Furie, B. (2003) *J. Biol. Chem.* **278,** 31297–31302
22. Freedman, S. J., Blostein, M. D., Baleja, J. D., Jacobs, M., Furie, B. C., and Furie, B. (1996) *J. Biol. Chem.* **271,** 16227–16236
23. Sugo, T., Mizuguchi, J., Kamikubo, Y., and Matsuda, M. (1990) *Thromb. Res.* **58,** 603–614
24. Mimuro, J., Mizukami, H., Ono, F., Madoiwa, S., Terao, K., Yoshioka, A., Ozawa, K., and Sakata, Y. (2004) *J. Thromb. Haemost.* **2,** 275–280
25. Morita, T., and Kisiel, W. (1985) *Biochem. Biophys. Res. Commun.* **130,** 841–847
26. Mimms, L. T., Zampighi, G., Nozaki, Y., Tanford, C., and Reynolds, J. A.

Therapeutic Effects of Hepatocyte Transplantation on Hemophilia B

Kohei Tatsumi,[1] Kazuo Ohashi,[2,3,4,5] Midori Shima,[1] Yoshiyuki Nakajima,[2] Teruo Okano,[3] and Akira Yoshioka[1]

Hepatocyte transplantation offers an alternative therapeutic approach in the treatment of liver-related diseases. Hemophilia B is a bleeding disorder lacking factor IX (FIX) production in the liver, and achieving more than 1% coagulation activity results in significant improvement in the quality of life of the patients. The aim of this study was to investigate the efficacy of hepatocyte transplantation in the mouse model of hemophilia B. We transplanted isolated normal mouse hepatocytes into the liver of FIX knock-out mice. In some recipient mice, additional hepatocyte transplantations were performed 15 days after the first transplant. The recipient plasma FIX activities increased at 1% to 2% and persisted throughout the experimental period. An additional increase was achieved by the repeated transplantation. Close correlation between FIX messenger RNA levels of the liver and plasma FIX activity levels was observed. These results demonstrate that hepatocyte transplantation can provide therapeutic benefits in the treatment of hemophilia B.

Keywords: Hepatocyte transplantation, Hemophilia B, Coagulation factor IX, Experimental transplantation.

(*Transplantation* 2008;86: 167–170)

Hemophilia B, a recessive X-chromosome linked congenital bleeding disorder, is caused by a failure in the production of coagulation factor IX (FIX) (*1*). The only treatments that are currently available are the replacement therapy with FIX concentrates from plasma-derived or recombinant protein sources (*2*). This treatment modality is inefficient and expensive, because of the requirement of life-long and frequent intravenous infusion of FIX concentrates. Although the gene therapy has been actively studied over the past decade to establish a novel therapy that could provide longer acting and safer production of FIX (*3*), recent clinical trials have yet to conclusively shown long-term therapeutic benefits (*4, 5*). One potential approach that may provide the FIX producing ability in hemophilia B is a whole liver transplantation, because FIX is predominantly produced in the liver (*6–8*). However, the establishment of organ transplantation as a common therapy is hampered by a worldwide shortage of donor livers. Provided that some portion of the donated liver can be used for the isolation of individual hepatocytes, this donor shortage would no longer be a major issue. This is an important point, because the cell type responsible for synthesizing coagulation FIX is the hepatocyte (*9*). Therefore, a cell-based therapy using isolated hepatocytes could provide a therapeutic approach in the treatment of hemophilia B. Hepatocyte transplantation has been recently performed in several countries for various inherited disorders of hepatic metabolism and acute liver failure (*10, 11*). In bleeding disorder, hepatocyte transplantation was applied in the clinics by Dhawan et al. (*12*), who described therapeutic benefits in two patients suffering with congenital factor VII deficiency. Our group has recently shown applying a tissue engineering approach using primary hepatocytes could successfully provide therapeutic effects in hemophilia A mice (*13*). However, the effect of hepatocyte transplantation to treat hemophilia B has yet to be experimentally documented in animals or in the clinics to the best of our knowledge. For this reason, this study was designed to investigate the efficacy of hepatocyte transplantation on hemophilia B.

Hepatocytes were isolated from C57Bl/6 wild-type mice using a collagenase perfusion method as previously described (*13–16*). The recipient FIX knock-out (FIX-KO) mice, syngeneic to donor mice (*17*), were transplanted with the isolated hepatocytes (1.5×10^6 cells in 200 μL) into the liver through the inferior pole of the spleen (n=25). As an experimental control, several FIX-KO mice received sham operation (n=7). To avoid excessive surgical procedure-related bleeding, all FIX-KO mice received intraperitoneal injection of 0.5 mL pooled normal mouse plasma 30 min before abdominal surgery (*18*). All procedures were successfully carried out without any issues related to bleeding and all of the mice survived throughout the experimental period. At days 5, 10, and 15, some of the mice were killed for histologic and messenger RNA (mRNA) analyses (n=7, 5, and 4, at each time point, respectively). All sham-operated mice were killed at day 15.

Blood samples were periodically obtained from retro-orbital plexus of the experimental mice. After anticoagulated with 0.1 volume of 3.8% sodium citrate, blood samples were centrifuged, and plasma samples were stored at −80°C until being analyzed. The plasma FIX activity (FIX:C) was quanti-

This work was supported by grants form AIDS Research from the Ministry of Health, Labor and Welfare of Japan (A.Y.) and grant-in-Aid (18591957) (K.O.) and Special Coordination Funds for Promoting Science and Technology (K.O., T.O.), and from the Ministry of Education, Culture, Sports, Science and Technology (MEXT), Japan.

[1] Department of Pediatrics, Nara Medical University, Kashihara, Nara, Japan.
[2] Department of Surgery, Nara Medical University, Kashihara, Nara, Japan.
[3] Institute of Advanced Biomedical Engineering and Science, Tokyo Women's Medical University, Shinjuku-ku, Tokyo, Japan.
[4] Department of Gastroenterological Surgery Tokyo Women's Medical University, Tokyo, Japan.
[5] Address correspondence to: Kazuo Ohashi, M.D., Ph.D., Institute of Advanced Biomedical Engineering and Science, Tokyo Women's Medical University, 8-1 Kawada-cho, Shinjuku-ku, Tokyo 162-8666, Japan.
E-mail: ohashi@abmes.twmu.ac.jp

Received 8 November 2007. Revision requested 11 December 2007.
Accepted 2 April 2008.

ISSN 0041-1337/08/8601-167
DOI: 10.1097/TP.0b013e31817b9160

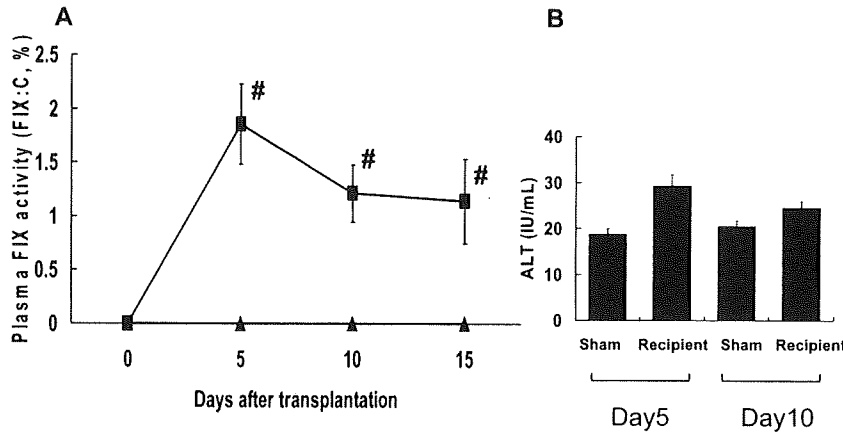

FIGURE 1. Plasma FIX activity (FIX:C) and alanine aminotransferase (ALT) levels of FIX-KO mice after hepatocyte transplantation. (A) FIX:C levels in plasma obtained from FIX-KO mice after hepatocyte transplantation (1.5×10^6 cells/mouse) into the liver (■; n=25, 18, and 13 at day 5, 10, and 15, respectively) or sham operation (▲; n=7 at all time points). Pooled normal mouse plasma was used as a standard. *#P* less than 0.05 between groups. (B) Plasma ALT levels of FIX-KO mice following hepatocyte transplantation (n=25 and 18) or sham operation (n=7) at day 5 and 10 of the experiment.

fied by 1-stage clotting assay based on the activated partial thromboplastin time using human FIX-deficient plasma. Normal mouse plasma was used as FIX:C standard. Each measurement was reported after subtraction of the preoperational baseline FIX:C levels. As a result, FIX:C of recipient mice increased to more than 1% and were stably maintained throughout the experimental period (Fig. 1A). The FIX:C levels were significantly higher in the recipient mice when compared with the levels in the sham-operated mice at every time point examined. At day 5, recipient mice showed a small, but insignificant increase in plasma alanine aminotransferase after the transplantation (n=25) compared with the sham-operated mice (n=7). The slight increase in the alanine aminotransferase levels were found to be declined back toward baseline levels at day 10 (Fig. 1B). These results indicated that hepatocyte transplantation into hemophilia B mice could provide a therapeutic effect by producing FIX from the engrafted donor hepatocytes without significant liver injuries.

Histologic detection of transplanted and engrafted hepatocytes was performed by fluorescence in situ hybridization analysis using mouse Y-chromosome specific probe on sections of female FIX-KO recipient liver that received male hepatocytes. The presence of hepatocytes with Y-chromosome signals were confirmed, indicating the transplanted hepatocytes engrafted into the liver parenchyma (figure not shown). It is also important to note that any cell fusion events were not observed.

To enhance the therapeutic production of FIX in the recipient mice, a repeat transplantation of isolated hepatocytes was performed 15 days after the initial procedure in some recipients by infusing 1.2×10^6 hepatocytes into the upper pole of the spleen (n=4). The other remaining recipients (n=5) were examined with only a single transplantation procedure. As shown in Figure 2, the FIX:C values of the FIX-KO mice at day 25 (10 days after the second transplantation) were 0.94%±0.05% and 1.85%±0.09% in the single- and double-transplanted recipient mice, respectively (P=0.038). Similar increases in FIX:C were also observed at day 35 (20 days after the second transplantation) in the double-transplanted group. These data clearly demonstrated that increasing therapeutic effects could be obtained with a repeated transplantation.

We also examined whether the engrafted hepatocytes were capable of transcribing FIX mRNA in the recipient mouse livers. Because shunting of the hepatocytes into the

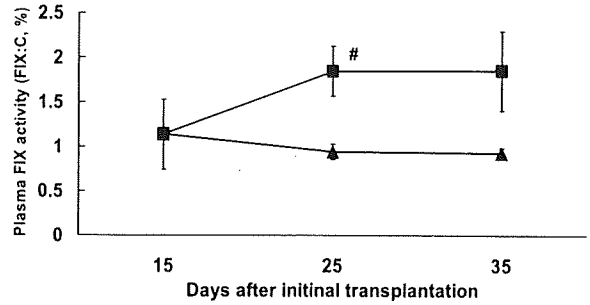

FIGURE 2. Effect of repeated hepatocyte transplantation on plasma FIX:C levels in hemophilia B mice. At day 15, some recipient FIX-KO mice received the second transplantation procedure using 1.2×10^6 hepatocytes (■; n=4), whereas remaining five recipient mice did not receive the second procedure (initial transplantation only, ▲; n=5). *#P* less than 0.05 between groups.

lung had been described in the previous experimental studies (*19*), we also investigated FIX mRNA levels in the lung. Total RNA was extracted from liver, lung, and spleen. Total RNA (1 μg) was reverse transcribed, and the first-strand complementary DNA samples were subjected to quantitative real-time polymerase chain reaction amplification for mouse FIX gene and β-actin gene. Serial dilutions of complementary DNAs of normal mouse liver were used to generate the standard amplification curves. As shown in Figure 3(A), an abundant level of FIX mRNA was detected in the liver, with even higher mRNA expression detected in the livers manipulated with the repeated transplantation. No FIX mRNA signal was detected in the lungs in any of the mouse groups. Incremental expression of FIX was detected in the spleen of single and double hepatocyte transplanted mice, but the levels were markedly lower compared with the livers. We examined the relationship between the FIX:C levels and the liver FIX mRNA levels, and found a direct positive correlation between the two parameters (R^2=0.7214) (Fig. 3B).

Furthermore, we assessed the development of neutralizing antibodies against FIX (FIX inhibitor) by Bethesda method using plasma obtained at killing (*20*). Detectable levels (>0.5 Bethesda U/mL) of FIX inhibitor was not measured

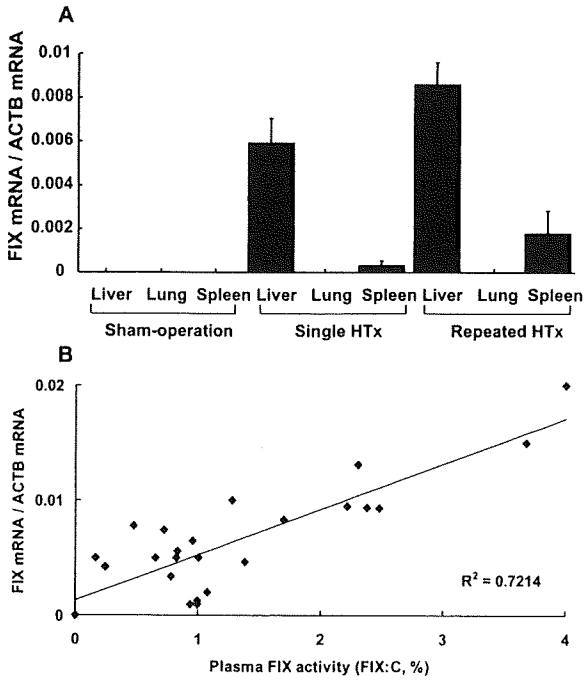

FIGURE 3. Functional engraftment of hepatocytes determined by FIX mRNA expression in the recipient mice. (A) Expression levels of FIX mRNA were determined by quantitative real-time reverse-transcriptase polymerase chain reaction in the liver, spleen, and lung from three experimentally manipulated groups: (1) single hepatocyte transplantation (n=21); (2) repeated hepatocyte transplantation (n=4); and (3) sham-operation (control) (n=7). Each of the FIX mRNA expression values were normalized to a housekeeping gene, β-actin. (B) Relationship between plasma FIX:C levels and FIX mRNA expression levels in the liver of recipient mice. The FIX:C levels of plasma obtained on the day of animal sacrifice were found to correlate with the relative FIX mRNA levels determined in (A) (R^2=0.7214).

in any of recipient mice. This demonstrates that bioengineered FIX produced from the transplanted hepatocytes does not associate with the development of FIX inhibitors.

To investigate the long-term engraftment of hepatocytes, we performed an another set of single transplantation experiment for 12 weeks (n=6), and confirmed long-term persistency of the increased FIX activities at 0.92%±0.22%, 0.78%±0.22%, 0.78%±0.22%, and 0.83%±0.17% at week 2, 4, 8, and 12, respectively.

The present study confirmed the proof-concept feasibility of hepatocyte transplantation as an alternative therapy to treat hemophilia B. The functional engraftment of transplanted hepatocytes within the recipient livers was confirmed by fluorescence in situ hybridization analyses, FIX mRNA expression, and the secretion of functional FIX into the blood circulation. To acquire the proper hemostatic activity, synthesized coagulation FIX requires several posttranscriptional modification steps within the hepatocytes, including cleavage and removal the prepro leader sequence of 46 amino-acids, and γ-carboxylation of the first 12 glutamic acid residues (*21*). For this reason, primary hepatocytes would be more appropriate for transplantation to produce coagulation factors in hemophilia B than other possible types of genetically modified cells expressing FIX.

Previous studies have shown that engrafted hepatocytes within the livers are able to proliferate in response to the regeneration signals occurred by surgical hepatectomy or chronic liver injuries (*22, 23*). Using primary hepatocytes, our group has developed several innovative approaches to create a functional liver system under the kidney capsule or in subcutaneous locations (*13, 15, 16, 24, 25*), and we have clearly demonstrated that these ectopically engrafted hepatocytes also possess the ability for proliferation (*13, 16, 26*). This would be a significant benefit in the use of these hepatocytes, because most of the adult hemophilia B patients presented with chronic hepatitis B and/or C viral infection as a result of treatments with blood-borne contaminated plasma-derived FIX concentrates. Although portion of the transplanted hepatocytes would be infected with hepatitis viruses in the mean time, it would be reasonable to speculate that engrafted hepatocytes will proliferate and expand, which would further increase the therapeutic effects.

In conclusion, the present studies described the feasibility and safety of hepatocyte transplantation as a treatment modality for hemophilia B. Current therapies to treat hemophilia have been confounded with problems, and the present findings represent an important step toward establishing an alternative therapeutic approach for the treatment of not only hemophilia, but other similar genetic disorders affecting the liver.

ACKNOWLEDGMENTS

The authors thank Yuichi Komai, Yuka Bessho, and Sanae Taminishi (Department of Pediatrics, Nara Medical University) for their technical assistance, and Dr. Frank Park (Medical College of Wisconsin) for his critical reading of the manuscript.

REFERENCES

1. Bolton-Maggs PH, Pasi KJ. Haemophilias A and B. *Lancet* 2003; 361: 1801.
2. Manco-Johnson MJ, Abshire TC, Shapiro AD, et al. Prophylaxis versus episodic treatment to prevent joint disease in boys with severe hemophilia. *N Engl J Med* 2007; 357: 535.
3. Nathwani AC, Davidoff AM, Tuddenham EG. Prospects for gene therapy of haemophilia. *Haemophilia* 2004; 10: 309.
4. Manno CS, Chew AJ, Hutchison S, et al. AAV-mediated factor IX gene transfer to skeletal muscle in patients with severe hemophilia B. *Blood* 2003; 101: 2963.
5. Manno CS, Pierce GF, Arruda VR, et al. Successful transduction of liver in hemophilia by AAV-Factor IX and limitations imposed by the host immune response. *Nat Med* 2006; 12: 342.
6. Gordon FH, Mistry PK, Sabin CA, et al. Outcome of orthotopic liver transplantation in patients with haemophilia. *Gut* 1998; 42: 744.
7. Ko S, Tanaka I, Kanehiro H, et al. Preclinical experiment of auxiliary partial orthotopic liver transplantation as a curative treatment for hemophilia. *Liver Transpl* 2005; 11: 579.
8. Merion RM, Delius RE, Campbell DA, Jr, et al. Orthotopic liver transplantation totally corrects factor IX deficiency in hemophilia B. *Surgery* 1988; 104: 929.
9. Boost KA, Auth MK, Woitaschek D, et al. Long-term production of major coagulation factors and inhibitors by primary human hepatocytes in vitro: perspectives for clinical application. *Liver Int* 2007; 27: 832.
10. Fisher RA, Strom SC. Human hepatocyte transplantation: Worldwide results. *Transplantation* 2006; 82: 441.
11. Ohashi K, Park F, Kay MA. Hepatocyte transplantation: Clinical and experimental application. *J Mol Med* 2001; 79: 617.
12. Dhawan A, Mitry RR, Hughes RD, et al. Hepatocyte transplantation for inherited factor VII deficiency. *Transplantation* 2004; 78: 1812.

13. Ohashi K, Waugh JM, Dake MD, et al. Liver tissue engineering at extrahepatic sites in mice as a potential new therapy for genetic liver diseases. *Hepatology* 2005; 41: 132.
14. Berry MN, Friend DS. High-yield preparation of isolated rat liver parenchymal cells: A biochemical and fine structural study. *J Cell Biol* 1969; 43: 506.
15. Ohashi K, Kay MA, Kuge H, et al. Heterotopically transplanted hepatocyte survival depends on extracellular matrix components. *Transplant Proc* 2005; 37: 4587.
16. Ohashi K, Kay MA, Yokoyama T, et al. Stability and repeat regeneration potential of the engineered liver tissues under the kidney capsule in mice. *Cell Transplant* 2005; 14: 621.
17. Lin HF, Maeda N, Smithies O, et al. A coagulation factor IX-deficient mouse model for human hemophilia B. *Blood* 1997; 90: 3962.
18. Snyder RO, Miao C, Meuse L, et al. Correction of hemophilia B in canine and murine models using recombinant adeno-associated viral vectors. *Nat Med* 1999; 5: 64.
19. Schneider A, Attaran M, Gratz KF, et al. Intraportal infusion of 99mtechnetium-macro-aggregrated albumin particles and hepatocytes in rabbits: Assessment of shunting and portal hemodynamic changes. *Transplantation* 2003; 75: 296.
20. Kasper CK, Pool JG. Letter: Measurement of mild factor VIII inhibitors in Bethesda units. *Thromb Diath Haemorrh* 1975; 34: 875.
21. Arruda VR, Hagstrom JN, Deitch J, et al. Posttranslational modifications of recombinant myotube-synthesized human factor IX. *Blood* 2001; 97: 130.
22. Kokudo N, Ohashi K, Takahashi S, et al. Effect of 70% hepatectomy on DNA synthesis in rat hepatocyte isograft into the spleen. *Transplant Proc* 1994; 26: 3464.
23. Zhang H, Miescher-Clemens E, Drugas G, et al. Intrahepatic hepatocyte transplantation following subtotal hepatectomy in the recipient: A possible model in the treatment of hepatic enzyme deficiency. *J Pediatr Surg* 1992; 27: 312.
24. Ohashi K, Marion PL, Nakai H, et al. Sustained survival of human hepatocytes in mice: A model for in vivo infection with human hepatitis B and hepatitis delta viruses. *Nat Med* 2000; 6: 327.
25. Yokoyama T, Ohashi K, Kuge H, et al. In vivo engineering of metabolically active hepatic tissues in a neovascularized subcutaneous cavity. *Am J Transplant* 2006; 6: 50.
26. Ohashi K, Yokoyama T, Yamato M, et al. Engineering functional two- and three-dimensional liver systems in vivo using hepatic tissue sheets. *Nat Med* 2007; 13: 880.

Successful *in vivo* propagation of factor IX-producing hepatocytes in mice: Potential for cell-based therapy in haemophilia B

Kohei Tatsumi[1], Kazuo Ohashi[2, 5], Miho Kataoka[3], Chise Tateno[3, #], Masaru Shibata[1], Hiroyuki Naka[1], Midori Shima[1], Michiyoshi Hisanaga[2], Hiromichi Kanehiro[2], Teruo Okano[5], Katsutoshi Yoshizato[3, 4, #], Yoshiyuki Nakajima[2], Akira Yoshioka[1]

[1]Department of Pediatrics, Nara Medical University, Nara, Japan; [2]Department of Surgery, Nara Medical University, Nara, Japan; [3]Yoshizato Project, Cooperative Link of Unique Science and Technology for Economy Revitalization (CLUSTER), Hiroshima Prefectural Institute of Industrial Science and Technology, Hiroshima, Japan; [4]Graduate School of Science, Hiroshima University, Hiroshima, Japan; [5]Institute of Advanced Biomedical Engineering and Science, Tokyo Women's Medical University, Tokyo, Japan

Summary

Cell-based therapies using isolated hepatocytes have been proposed to be an attractive application in the treatment of haemophilia B due to the normal production of coagulation factor IX (FIX) in these particular cells. Current cell culture technologies have largely failed to provide adequate isolated hepatocytes, so the present studies were designed to examine a new approach to efficiently proliferate hepatocytes that can retain normal biological function, including the ability to synthesize coagulation factors like FIX. Canine or human primary hepatocytes were transplanted into urokinase-type plasminogen activator-severe combined immunodeficiency (uPA/SCID) transgenic mice. Both donor hepatocytes from canines and humans were found to progressively proliferate in the recipient mouse livers as evidenced by a sharp increase in the circulating blood levels of species-specific albumin, which was correlated with the production and release of canine and human FIX antigen levels into the plasma. Histological examination confirmed that the transplanted canine and human hepatocytes were able to proliferate and occupy >80% of the host livers. In addition, the transplanted hepatocytes demonstrated strong cytoplasmic staining for human FIX, and the secreted coagulation factor IX was found to be haemostatically competent using specific procoagulant assays. In all, the results from the present study indicated that developments based on this technology could provide sufficient FIX-producing hepatocytes for cell-based therapy for haemophilia B.

Keywords

Haemophilia A/B, haemophilia therapy, coagulation factors, hepatology

Thromb Haemost 2008; 99: 883–891

Introduction

Haemophilia B is a rare X-chromosome-linked recessive bleeding disorder, caused by a failure in the production of functional coagulation factor IX (FIX), and this disease affects ~1 in 30,000 males (1, 2). The main clinical manifestation of this disease is similar to haemophilia A (factor VIII deficiency), and under severe conditions the affected patient can be found to have unpredictable, recurrent, spontaneous bleeding in various areas, including soft tissues, major joints and occasionally in internal organs. In these circumstances, the onset and progression of chronic haemoarthropathy leads to a marked disruption in the physical and social aspects of the affected patients. Standard treatment for haemophilia B is either on-demand or prophylactic therapy with plasma-derived or recombinant human FIX concentrates. This type of treatment requires frequent intravenous infusion, which can be a potential biohazard from blood-borne viral infections to the patient if the infusate is derived from a heterogeneous population of human blood. In addition, the high cost of commercial concentrates and the life-long requirement for replacement therapy can have a significant impact on economic resources. In an attempt to resolve these difficulties, longer acting

Correspondence to:
Kazuo Ohashi, MD, PhD
Institute of Advanced Biomedical Engineering and Science
Tokyo Women's Medical University
8–1 Kawada-cho, Shinjuku-ku, Tokyo, 162–8666, Japan
Tel.: +81 3 3353 8111, ext 66214, Fax: +81 3 3359 6046
E-mail: ohashi@abmes.twmu.ac.jp

Present address: PhoenixBio Co. Ltd. Hiroshima, Japan.

Financial support:
This study was supported in part by The Leading Projects (K.O. and T.O.) and Grant-in-Aid (no. 18591957 to K.O.) from the Scientific Research from the Ministry of Education, Science, Sport and Culture of Japan, grants for AIDS Research from the Ministry of Health, Labor and Welfare of Japan (A.Y.), and grant for CLUSTER (K.Y.).

Received September 12, 2007
Accepted after major revision March 12, 2008

Prepublished online April 9, 2008
doi:10.1160/TH07-09-0559

and safer therapeutic strategies have been investigated. For example, gene therapy using viral vectors has been extensively studied in the past decade (3), and although therapeutic and long-term efficacy has been demonstrated in animal models (4–12), clinical trials have not conclusively shown long-term therapeutic benefit (13, 14). It seems likely, therefore, that alternate therapeutic options will need to be developed.

Recent clinical success with liver transplantation in haemophilia has encouraged further investigation into cell-based therapies (15–17). In haemophilia B patients, elevations in biologically active FIX levels from <1.0% to >1.0%, can alter the phenotype from severe to moderate resulting in a marked improvement in the symptomology and quality of life (1). Coagulation FIX is synthesized in hepatocytes (18), and so cell-based therapies using isolated hepatocytes could provide therapeutic potential. Hepatocytes also produce other coagulation factors, such as factors VII and VIII (19–24), and it may be that this type of treatment could have broader applications to not only haemophlia B, but other coagulation deficiencies. Recently, we have adopted several approaches to bioengineer functional liver tissue *in vivo* (25–30). We have demonstrated that isolated hepatocytes transplanted under the kidney capsule in haemophilia A mice produced therapeutic plasma FVIII activity and corrected the phenotypic defect (28). Dhawan et al. (31) also recently described the therapeutic benefits of hepatocyte transplantation in congenital factor VII deficiency, and the relative technical simplicity of cell-based therapy may offer a significant and technological advantage.

One of the major hurdles in establishing this type of therapy is the limited availability of biologically functional hepatocytes. At present, the number of donor livers remains severely restricted and even if they are available, these livers are frequently of marginal quality (32). Current procedures for the culture of primary hepatocytes do not appear to support extensive cell proliferation (33), so methods to circumvent this problem have recently been studied, but their role to treat haemophilia were not examined. Isolated hepatocytes were genetically modified via transfection with an immortalizing gene, such as simian virus 40 large T antigen, to promote long-term survival (34), but FIX gene expression and production was not investigated. Although the genetic manipulation of hepatocytes can be achieved following isolation *in vitro*, this type of approach to promote hepatocyte proliferation is not a trivial matter *in vivo*. Towards this end, methods to provide proliferative stimuli has been studied *in vivo*, such as a reduction in existing liver mass, or alternatively in a condition where there is likely to be a selective advantage for transplanted cells to proliferate (26, 28). Due to these limitations, we investigated a different method to isolate and proliferate hepatocytes that can retain the hepatic machinery to sustain the synthesis of coagulation factors, such as FIX. In the present study, we studied whether transplantation of canine or human primary hepatocytes into urokinase-type plasminogen activator-severe combined immunodeficiency (uPA/SCID) transgenic mice could enhance the production of coagulation factor IX. The uPA/SCID mouse has been previously shown to have hepatic parenchymal cell damage, which results in the continuous release of regenerative stimuli (35), so we believed that the hepatic environment may be more conducive to the engraftment of *in vitro* isolated hepatocytes. The functionality of the transplanted hepatocytes was assessed in terms of FIX mRNA and protein production and biological activity as a means to treat haemophilia B.

Materials and methods

Animals

Normal beagles were purchased from Oriental BioService, Inc. (Kyoto, Japan). C57BL/6 mice were purchased from Jackson Laboratory (Bar Harbor, ME, USA). uPA/SCID mice were generated at Hiroshima Prefectural Institute of Industrial Science and Technology (Higashihiroshima, Hiroshima, Japan) as described previously (35). Genotyping for the presence of the uPA transgene in the SCID mice was confirmed by polymerase chain reaction (PCR) assay of isolated genomic DNA as described previously (35, 36). Experimental protocols were developed in accordance with the guidelines of the local animal committees located at both Hiroshima Prefectural Institute of Industrial Science and Technology and Nara Medical University.

Hepatocyte isolation

Canine hepatocytes were isolated from livers (~100 g piece) harvested from two normal beagles (Dog 1: 7-year-old male and Dog 2: 1-year-old female) by a two-step perfusion method using 0.05% collagenase (Collagenase S1, Nitta Gelatin, Osaka, Japan) as described previously (25, 27). Cells were then filtered and hepatocytes were separated from non-parenchymal cells by sequential low speed centrifugation at 50 x g followed by Percoll (Percoll™, Amersham Biosciences, Uppsala, Sweden) isodensity centrifugation. The viabilities of the isolated canine hepatocytes were 96.5% and 98.0% as determined by the trypan blue exclusion test. Hepatocytes were kept at 4°C until transplantation. Human hepatocytes, isolated from a one-year-old white male and a six-year-old Afro-American female, were purchased from In Vitro Technologies (Baltimore, MD, USA). The cryopreserved hepatocytes were thawed and suspended in transplant medium (35, 37). The viabilities of thawed human hepatocytes were determined to be 64.4% and 49.2%, respectively.

Transplantation of hepatocytes for the creation of canine- or human-chimeric mice

One day prior to transplantation and one week after transplantation, the uPA/SCID mice, 20 to 30 days old, received intraperitoneal injections of 0.1 mg of anti-asialo GM1 rabbit serum (Wako Pure Chemical Industries Ltd., Osaka, Japan) to inhibit recipient natural killer cell activity against the transplanted hepatocytes. Viable canine- (1.0×10^6) or human- (0.75×10^6) hepatocytes were transplanted using an infusion technique into the inferior splenic pole in which the transplanted cells flow from the spleen into the liver via the portal system. After transplantation, the uPA/SCID mice were treated with nafamostat mesilate to inhibit complement factors activated by canine or human hepatocytes as previously described (35).

Measurement of plasma levels of albumin, FIX antigen and FIX activity

Periodically, retroorbital bleeding was performed in recipient mice, and the blood was collected in a tube containing 0.1 vol

3.8% sodium citrate. Plasma samples were stored at –80°C until analyzed. To assess the proliferating status of transplanted canine hepatocytes, we determined the plasma levels of canine albumin in the recipient plasma by ELISA using primary goat anti-dog albumin and secondary HRP-conjugated goat anti-dog albumin antibodies (Bethyl Laboratories Inc., Montgomery, TX, USA), respectively. For the assessment of proliferation in transplanted human hepatocytes, we similarly measured the blood levels of human albumin by ELISA (Human Albumin ELISA Quantitation kit, Bethyl Laboratories Inc.). The proportion of proliferating donor hepatocytes in the recipient liver (repopulation rate) was determined based on blood albumin levels (35, 38). Human and canine FIX antigen (FIX:Ag) were measured in recipient plasma by ELISA (Asserachrom IX:Ag, Diagnostica Stago, Asnières, France). Human FIX:Ag levels were measured according to the instructions provided by the manufacturer, and canine FIX:Ag levels were quantified by elongating the enzymatic color reaction step. No cross-reactivity with pooled mouse plasma was observed in this ELISA. FIX activity (FIX:C) was measured by one-stage clotting assay based on the activated partial thromboplastin time using human FIX-deficient plasma (bioMerieux Inc., Durham, NC, USA). Pooled canine plasma collected from 75 normal dogs, and normal human plasma (Verify 1, bioMerieux Inc.) were used as reference standards.

Immunohistochemistry for albumin and FIX

Formalin-fixed, paraffin-embedded liver sections from mice transplanted with canine hepatocytes were sectioned and incubated with a primary goat antibody against canine albumin (Bethyl Laboratories Inc.) at a dilution of 1:1,000. The bound antibody was detected by the avidin-biotin complex immunoperoxidase technique using an ABC Elite kit (Vector Laboratories, Burlingame, CA, USA) followed by developing with DAB (3, 3'-diaminobenzine tetrahydrochloride). Expression of human FIX in recipient mice was determined by immunofluorescent staining of frozen liver sections embedded in O.C.T compound

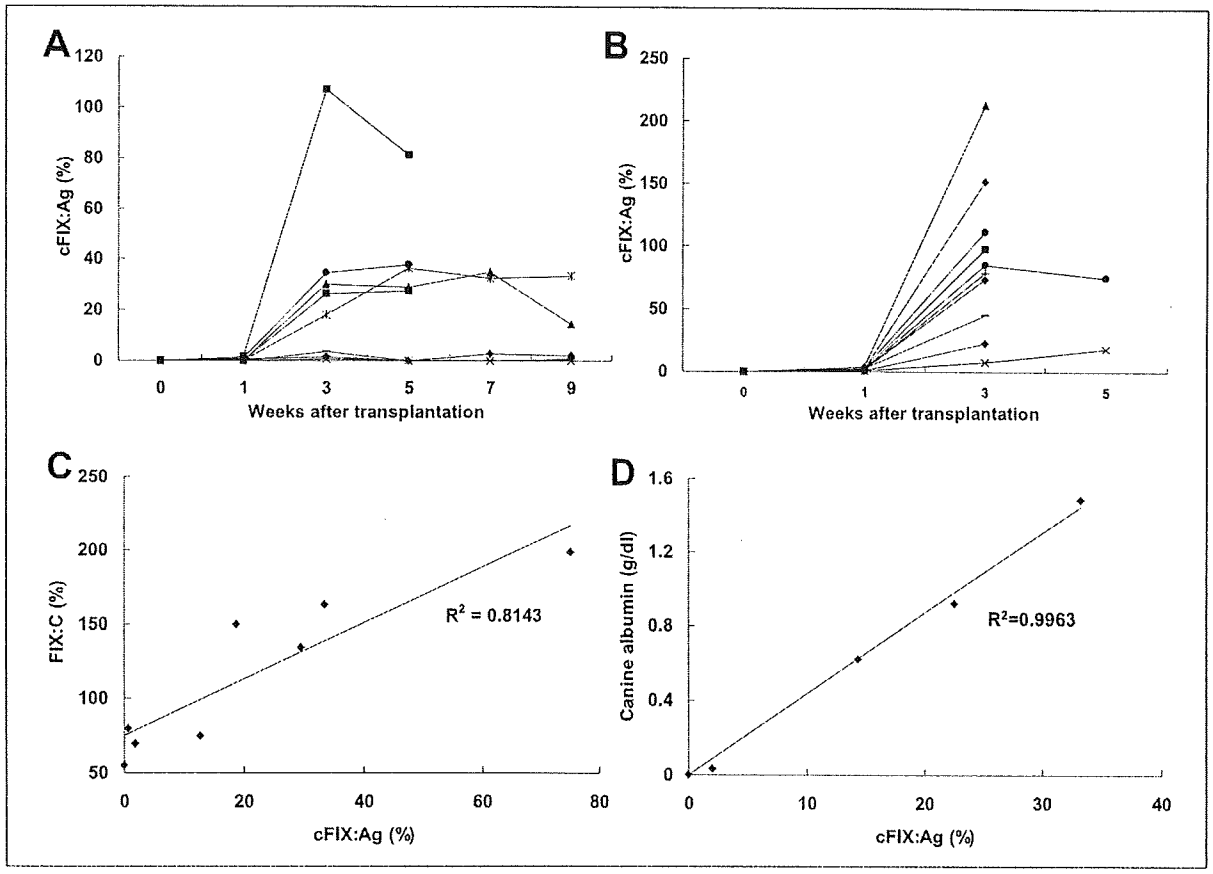

Figure 1: Proliferation of transplanted canine hepatocytes in uPA/SCID mouse livers assessed by recipient plasma analyses. A, B) Plasma canine factor IX (FIX) antigen (cFIX:Ag) levels in uPA/SCID mice after transplantation of hepatocytes isolated from a seven-year-old dog (A) and a one-year-old dog (B) (n=8, 10 in A and B, respectively) (% of pooled normal canine plasma). C) Relationship between total plasma FIX coagulation activity (FIX:C; reflecting both murine and canine FIX activities) (% of normal human plasma) and plasma cFIX:Ag levels of uPA/SCID mice transplanted with canine hepatocytes. D) Relationship between plasma canine albumin concentrations and plasma cFIX:Ag levels of uPA/SCID mice transplanted with canine hepatocytes.

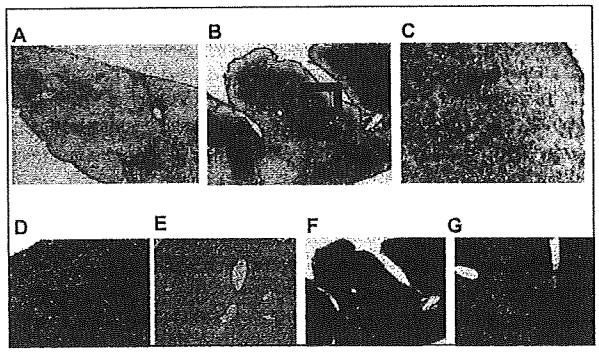

Figure 2: Mouse liver chimerism with proliferated canine hepatocytes. A-E) Immunohistochemical staining of canine albumin in liver sections of uPA/SCID mice transplanted with canine hepatocytes. Representative photomicrographs from a recipient mouse with low plasma cFIX:Ag (2.0% of normal canine plasma) (A) and a mouse with high plasma cFIX:Ag (33.2% of normal canine plasma) (B). C) Higher magnification view of the area outlined in (B). Canine albumin staining of positive control (normal dog liver) (D) and negative control (non-transplanted uPA/SCID mouse liver) (E) indicate the antibody used is specific for canine albumin. F, G) Hematoxylin and Eosin staining on the serial sections of mouse liver from (B). Ca, transplanted canine hepatocytes; Mu, recipient murine liver tissue. Original magnifications, ×40 (A, B, F), ×100 (D,E), and ×200 (C, G).

(Sakura Finetek, Torrance, CA, USA). The sections were incubated overnight at 4°C with the goat anti-human FIX antibody (Affinity Biologicals, Hamilton, ON, Canada) followed by Alexa Fluor 555 rabbit anti-goat IgG (Molecular Probes, Carlsbad, CA, USA) for 60 minutes. Stained sections were subsequently imaged using an Olympus BX51 microscope (Tokyo, Japan) and photographed using an Olympus DP70 digital camera with DP controller and DP manager computer software.

Quantitative real-time PCR

Total RNA was extracted from the liver of all recipient mice, and normal human and canine liver samples using the RNeasy Mini Kit (Qiagen, Hilden, Germany). Normal human liver tissue portions were obtained from surgical specimens at liver surgery for metastatic liver tumours after acquiring written informed consent for the experimental use of harvested liver samples. Extracted RNA (1 μg) was reverse transcribed using oligo $d(T)_{16}$ primers and Omniscript RT Kit (Qiagen). First-strand cDNA samples were subsequently subjected to PCR amplification using the PRISM 7700 Sequence Detector (Applied Biosystems Japan Ltd., Tokyo, Japan). Canine glyceraldehydes-3-phosphate dehydrogenase (GAPDH) and canine FIX sequences were detected using the following primers. The PCR primers for canine GAPDH sequence were forward, 5'CCCCACCCCCAATGTATCA3', reverse, 5'GTCGTCATATTTGGCAGCTTTCT3', and probe, 5'TGTGGATCTGACCTGCCGCCTG3'.
The primers for canine FIX sequence were forward, 5'GTTGTTGGTGGAAAAGATGCC3', reverse, 5'TGCATCAACTTTCCCATTCAAA3', probe, 'CCAGGTCAATTCCCTTGGCAGGTCC3'. TaqMan probes and primers for human sequences were Hs99999905_m1 (GAPDH) and Hs00609168_m1 (FIX) (TaqMan Gene Expression Assay, Applied Biosystems). The relative RNA copy numbers of canine FIX and human FIX in each transplanted mouse were calculated in terms of canine FIX / canine GAPDH or human FIX / human GAPDH expression ratio, respectively. RNA expression of murine FIX and murine GAPDH, combined with cDNA synthesis and real-time PCR using TaqMan probes, Mm99999915_g1 (murine GAPDH) and Mm01308427_m1 (murine FIX) (Applied Biosystems), were similarly assessed in hepatectomy experiments (see below).

Hepatectomy experiment

For the purpose of investigating the FIX mRNA expression during liver regeneration, liver proliferation stimuli was induced by performing a 70% partial hepatectomy on C57BL6 wild-type mice (n=6) as described previously (39). The resected liver lobes were used as our control for a liver sample under quiescence while the remnant liver lobes removed two days after hepatectomy were used as our proliferating samples. Mouse FIX mRNA and mouse GAPDH mRNA expression was assessed on both quiescent and proliferating liver samples as described above.

Statistical analysis

Significant differences were tested by the Wilcoxon t-test between paired groups and by the Mann-Whitney U-test between unpaired groups. Differences between three or more groups were tested by the Kruskal Wallis H-test. If the probability (p) value was less than 0.05, the Mann-Whitney U-test with Bonferroni correction was used to compare each individual group with the appropriate control. All statistical analyses were performed using Excel (Microsoft) with ystat2006 software (Igakutosyo-syuppan, Tokyo, Japan). $P<0.05$ was considered significant.

Results

Proliferation of FIX-producing canine hepatocytes in uPA/SCID mouse livers

Canine hepatocytes isolated from a seven-year-old and a one-year-old beagle were transplanted into uPA/SCID mice (n=8 and 10, respectively). Canine FIX:Ag was detected in the plasma of five out of eight mice three weeks after transplantation with the isolated hepatocytes from the seven-year-old beagle. In four out of the five mice, the FIX:Ag levels reached between 20–40% of normal canine plasma levels for FIX:Ag (Fig. 1A). One transplanted mouse was detected to have nearly 100% of normal canine plasma FIX:Ag levels. In general, the uPA/SCID mice that received hepatocytes from the one-year-old beagle demonstrated a greater rise in the circulating canine FIX:Ag, and 70% of the mice (7 out of 10) showed levels greater than 50% of normal levels three weeks after transplantation (median: 81.8%; Fig. 1B).

Plasma FIX:C was measured using a one-stage clotting assay. The FIX:C of normal canine pooled plasma and untreated uPA/SCID mouse plasma (n=4) was approximately 200% and 50% of normal human plasma, respectively. The FIX:C in the recipient uPA/SCID mice with high canine FIX:Ag levels was greater than in untreated mice or recipient uPA/SCID mice with low FIX:Ag levels ($R^2=0.8143$) (Fig. 1C). These observations confirmed that the secreted FIX protein had functional coagulation activity.